National Library of Canada
Acquisitions and Bibliographic Services Branch
395 Wellington Street
Ottawa, Ontario
K1A 0N4

Bibliothèque nationale du Canada
Direction des acquisitions et des services bibliographiques
395, rue Wellington
Ottawa (Ontario)
K1A 0N4

Your file Votre référence

Our file Notre référence

NOTICE

The quality of this microform is heavily dependent upon the quality of the original thesis submitted for microfilming. Every effort has been made to ensure the highest quality of reproduction possible.

If pages are missing, contact the university which granted the degree.

Some pages may have indistinct print especially if the original pages were typed with a poor typewriter ribbon or if the university sent us an inferior photocopy.

AVIS

La qualité de cette microforme dépend grandement de la qualité de la thèse soumise au microfilmage. Nous avons tout fait pour assurer une qualité supérieure de reproduction.

S'il manque des pages, veuillez communiquer avec l'université qui a conféré le grade.

La qualité d'impression de certaines pages peut laisser à désirer, surtout si les pages originales ont été dactylographiées à l'aide d'un ruban usé ou si l'université nous a fait parvenir une photocopie de qualité inférieure.

Canada

Studies on Antifungal and Antitumor Fungal Metabolites; Isolation, Characterization and Applications

Xiao-Jin Xu

A Thesis

in

the Department

of

Chemistry and Biochemistry

Presented in Partial Fulfilment of the Requirements

for the Degree of Master of Science

at Concordia University

Montreal, Quebec

Canada

November 1993

ISBN 0-315-90896-3

Canada

ABSTRACT

Studies on Antifungal and Antitumor Fungal Metabolites: Isolation, Characterization and Applications

Xiao-Jin Xu

Fusarium lateritium is a natural antagonist of the serious plant pathogen *Eutypa armeniacae* which is associated with sapwood necrosis. Two novel biologically active compounds, 2(1-hydroxyethyl)-4(3H)quinazolinone and 2-acetyl-4(3H)-quinazolinone, and three antifungal metabolites, the enniatins B, B_1, A_1, were isolated and characterized.

In addition, the metabolite mixture produced by a *Trichoderma* fungus was shown to exhibit strong cytotoxic activity against murine leukemia cells and human solid tumor cells. A novel α-pyrone, was isolated from this organism and its structure was characterized.

To my loving parents Ru-Pei and Ben-An,
for their emotional support and understanding.

Acknowledgements

I would like to thank my supervisor Professor Youla Tsantrizos for her endless encouragement, support, help and guidance.

A special thanks to Dr. Françoise Sauriol for her help and advice with the 500 MHz NMR spectra.

I would like to thank Professor Paul Widden for providing us with the *Trichoderma* fungus and his helpful advice on microbiology.

I also would like to thank Dr. Theresa Allen (Department of Pharmacology, University of Alberta), Dr Brian Leyland-Jones (Department of Oncology, Faculty of Medicine, McGill University) for their contributions to the bioassay on murine leukemic cells and human solid tumor cells in this thesis.

I would like to thank Dr. Orval Mamer for his help on mass spectrometry.

I would like to thank Professor Lawrance Colebrook for his advice on NMR techniques and Professor Paul Joyce for his advice on biochemical techniques and the use of equipment in his laboratory.

I would also like to thank our glass blower, Mr. Chris Kowalewski for all his help.

I would thank my aunt Ru-Yun, uncle Herb and cousin Tan-Hui for their love, support and help in so many ways.

I would like to thank, in a very special way, Parsa Famili, Fei Zhou, Selena Boothroyd, Thea Scantlebury and Jackie Lunetta for their friendship and helpful discussions.

Table of Contents

List of Figures

List of Tables

CHAPTER 1

INTRODUCTION

The term "natural product" is commonly reserved for those organic compounds of natural origin which are non-essential to the plant or microorganism which is producing them.[1] Man has used natural products, albeit as crude extracts, since the dawn of time. For example, 5100 years ago, the Chinese Emperor Shen Nung recorded traditional Chinese medicines which were used at that time in his book called *Pentsao*. One of them is Ch'ang Shan, the root of the *Dichroa febrifuga* plant, which was prescribed for fevers.[2] This plant produces the alkaloids, febrifugine (**1**) and isofebrifugine (**2**), which are now used for the treatment of malaria.

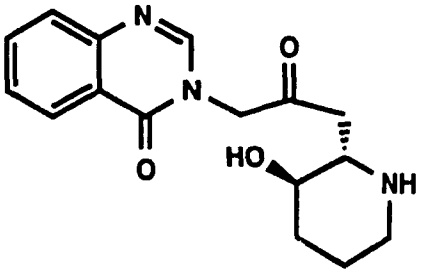

Febrifugine (1)

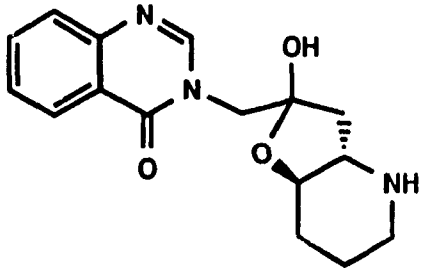

Isofebrifugine (2)

Another such example is opium (poppy juice); used as an analgesic in the third century B.C. and now to extract morphine (**3**), a potent analgesic, and codeine (**4**) which is commonly prescribed as a cough suppressant.

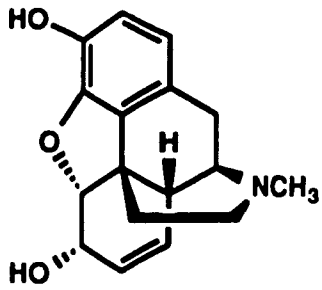

Morphine (3)

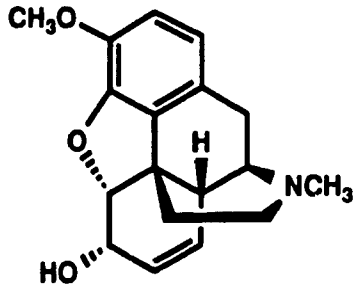

Codeine (4)

Microbial metabolites are another major source of natural products. They play an important role in everyday life for the commercial production of industrial, medicinal and agricultural compounds. For example, in the food industry, they are used to produce ergosterol (**5**) which upon irradiation gets converted to Vitamin D_2 (**6**) commonly added in milk (**Fig.1**). [3]

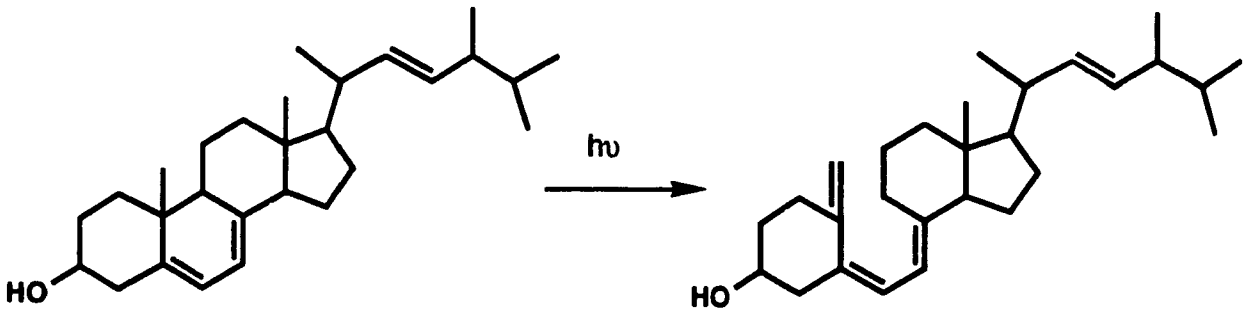

Ergosterol (5) **Vitamin D_2 (6)**

Figure 1: Synthesis of Vitamin D (6) from Ergosterol (5)

In medicine, since the discovery of penicillin in 1928 by Sir Alexander Fleming, thousands of antibacterial, antifungal and antitumor agents have been isolated from various bacteria and fungi. Among the most recent examples are such potent antitumor metabolites as calicheamicin γ_1 (**7**),[4] produced by *Micromonospora echinospora ssp. calichensis* and taxol (**8**) from *Taxomyces*

andreanae.[5] In addition to the potential value of such natural products which stems from their biological properties, their extraordinary molecular structure makes them fascinating intellectual challenges for a variety of synthetic and structural studies in organic chemistry.

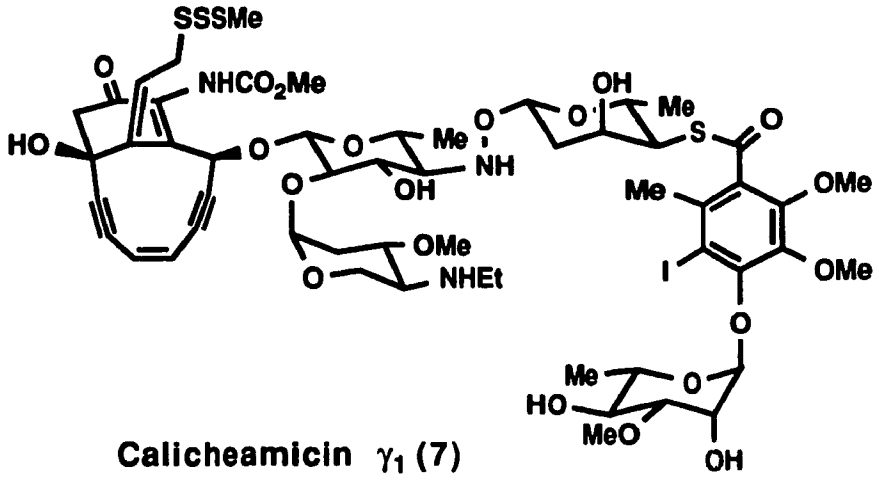

Calicheamicin γ_1 (7)

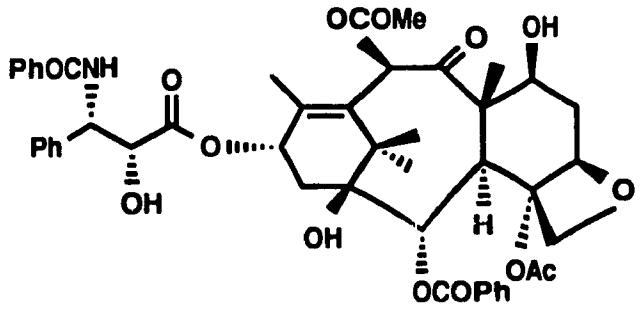

Taxol (8)

For example, a large number of studies have been published on the calicheamicins and other enediyne antitumor antibiotics (e.g., esperamicins[6] and dynemicin A[7]). Their common structural feature is a macrocyclic ring containing a conjugated enediyne system embedded in their skeletons (**Fig.2**).[8] It is believed that the enediyne moiety partially inserts into the minor

groove of DNA and then undergoes a reaction with either a thiol or NADPH which reduces the trisulfide to the corresponding thiolate (**9**).[9,10,11] Michael addition of this thiolate into the α,β-unsaturated ketone gives the dihydrothiophene (**10**) in which the hybridization of the bridgehead carbon has changed from sp^2 to sp^3. This allows the two triple bonds to interact with each other (cd distance changes from 3.35 Å to 3.16 Å) and undergo a Bergman rearrangement to give the activated calicheamicins benzenoid diradical (**11**).[12] The diradical species is capable of abstracting hydrogen atoms from DNA to give compound **12**, and DNA radicals react with molecular oxygen leading to double strand cleavages (**Fig.2**).

In recent years, the applications of natural products in agriculture have become an important aspect of scientific research. The "Bt" toxin is a good example; "Bt" are the initials for the bacterium *Bacillus thuringiensis kurstaki* which is now a commercially available biological insecticide. This bacterium produces a mixture of glycoproteins which are selectively toxic to certain insect larvae, mainly of the lepidopteran and dipteran species.[13] Unfortunately, the purified toxins are very sensitive to sun light. It is now known that Bt toxic proteins have a binding function (which determines what insect species they can effect) and a larvicidal function. The binding function varies from one Bt strain to another and the larvicidal function is about the same in all toxins. Brian Frederici and his colleagues at University of California fused two different Bt proteins together and they found that the chimeric protein was toxic to a wider range of insects than before.[14] The gene coding for these proteins was later inserted into various crop plants in order to enable them to produce similar proteins. These transgenic plants were found to be as resistant to insects as the natural control plants which had been sprayed with common synthetic insecticides.[15]

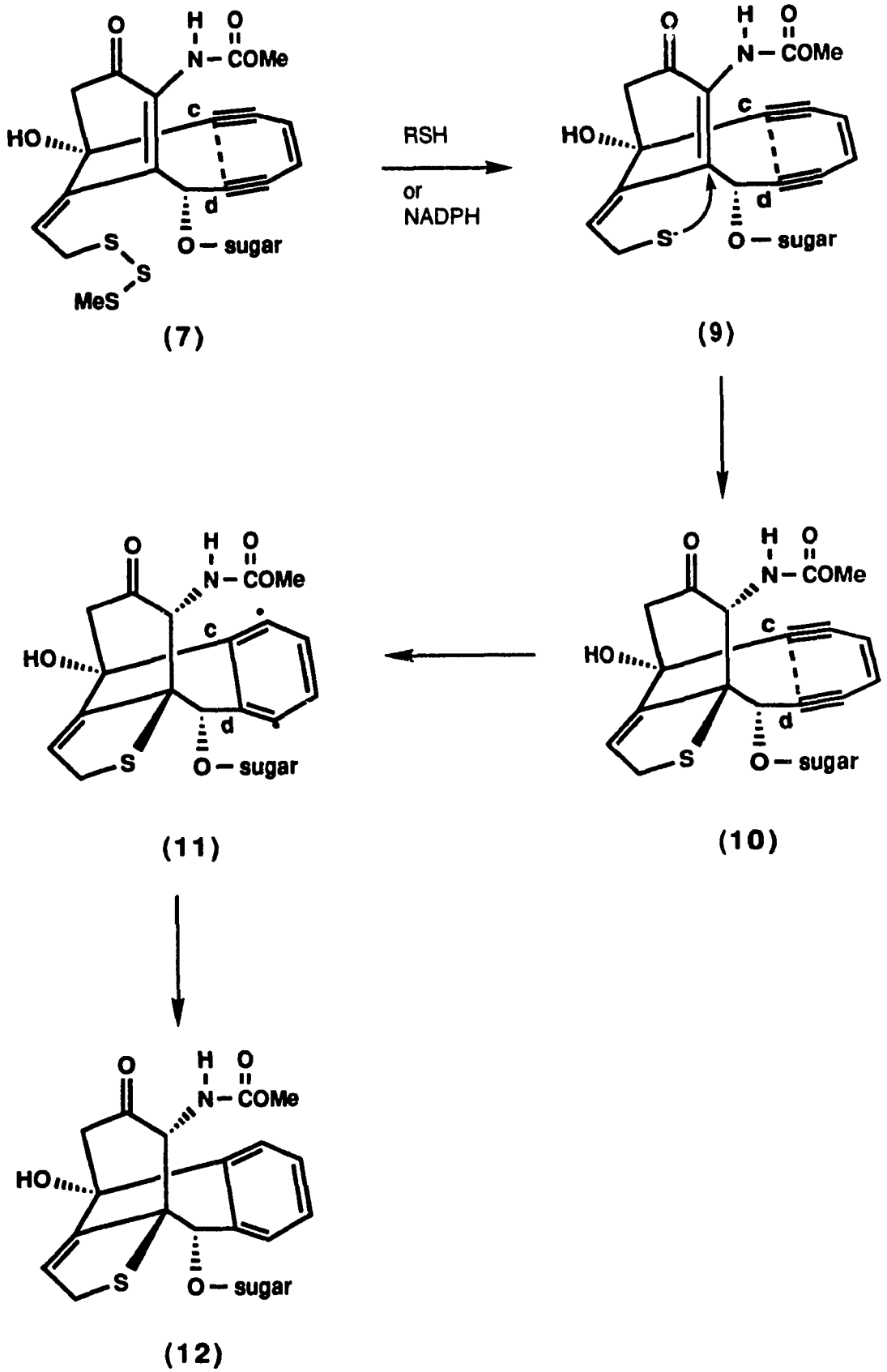

Figure 2: Mechanism of the DNA-Cleaving Action of Calicheamicin γ1 (7)

However, not all natural products are of potential therapeutic or commercial value. In fact, some microbial metabolites have been recognized as a serious threat to human and animal health. These metabolites are associated with acute and chronic toxicity, cytotoxicity and mutagenicity.

For example, aflatoxin B_1 (**13**) is one of the most common mycotoxins which is often found as a contaminant in food. The planar structure of the molecule allows it to intercalate into the double-strand of DNA. The subsequent mechanism of its action is known to involve activation of the isolated double-bond (on its dihydrobisfuran moiety) to an epoxide (**14**), followed by covalent bond formation between this metabolite and the N-7 of a guanine residue on the DNA (**15**) (**Fig.3**).[16] The cytotoxic effects of aflatoxins are most pronounced in tissues of the liver and kidneys.

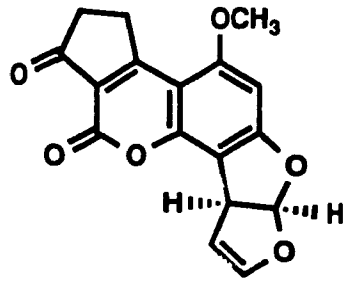

Aflatoxin B_1 (13)

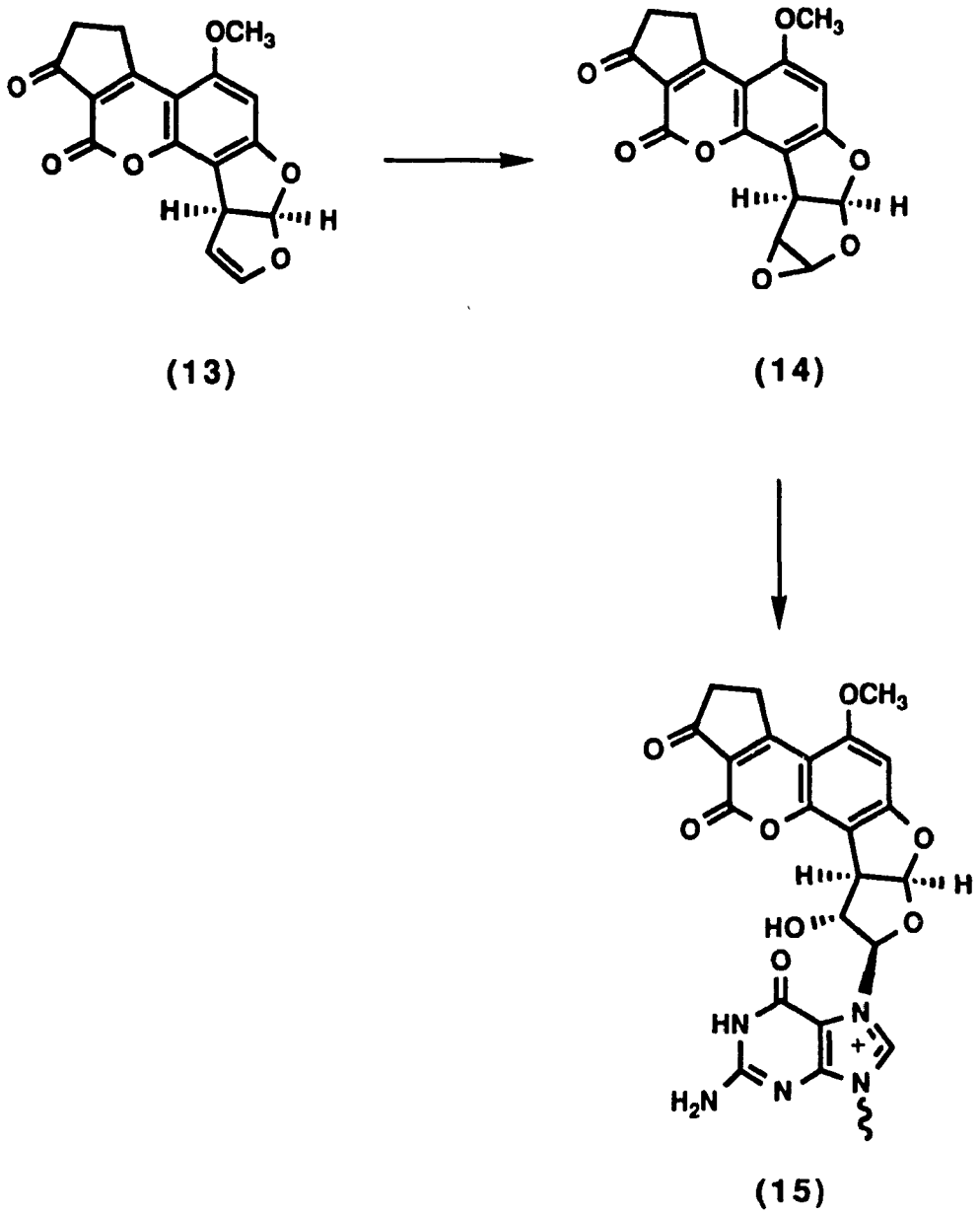

Figure 3: Mechanism of Action of Aflatoxin B_1 (13)

Given the important role of natural products in organic and medicinal chemistry, as well as biochemistry, the main object of this thesis was to investigate the biologically active metabolites produced by the two fungi: *Fusarium lateritium* Nees and a new member of the *Trichoderma* species.

F. lateritium is a natural antagonist of the serious plant pathogen *Eutypa armeniacae* which is associated with sapwood necrosis. Two novel biologically active compounds, 2(1-hydroxyethyl)-4(3H)quinazolinone(**16**) and 2-acetyl-4(3H)-quinazolinone(**17**), and three antifungal metabolites, the enniatins B (**18**), B_1 (**19**), A_1 (**20**) were isolated and characterized.

The metabolite mixture produced by the *Trichoderma* fungus exhibits strong cytotoxic activity against murine leukemia cells and human solid tumor cells. The α-pyrone **21**, a novel natural product, was isolated from this organism and its structure was characterized.

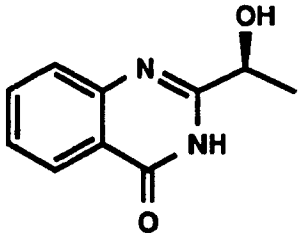

(16)

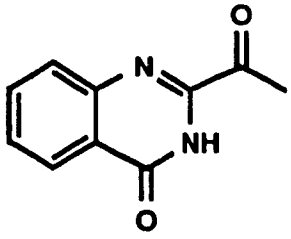

(17)

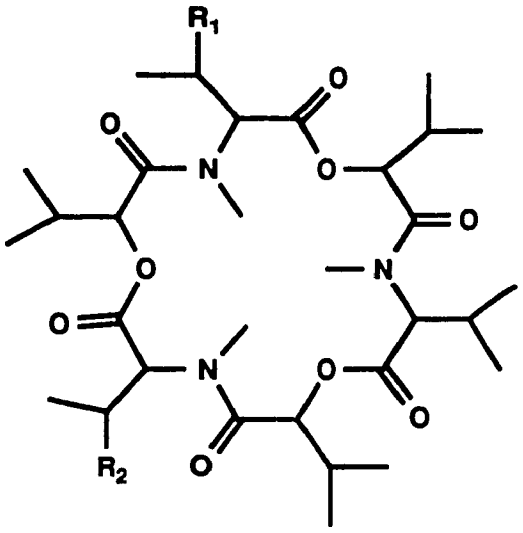

(18) $R_1=R_2=CH_3$

(19) $R_1=CH_2CH_3$, $R_2=CH_3$

(20) $R_1=R_2=CH_2CH_3$

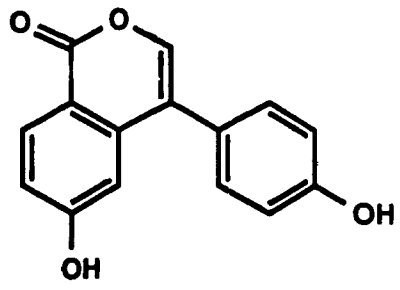

(21)

CHAPTER 2

Novel Quinazolinones and Enniatins from *Fusarium lateritium* Nees

2.1 Introduction:

In 1983, Carter[17a] described the use of *Fusarium lateritium* Nees macroconidia as a biofungicide for the protection of commercial apricot orchards from *Eutypa armeniacae* infections.[17] *E. armeniacae* is an aggressive plant pathogen associated with sapwood necrosis (commonly known as "dieback disease") in fruit trees, grapevines and ornamental plants around the world.[18] Thus, an investigation into the metabolites of *F. lateritium* which exhibit antifungal activity against *E. armeniacae* was undertaken.

A biologically active mixture of metabolites was obtained from *F. lateritium* cultures grown on solid Czapex-Dox plus yeast medium. The subsequent bioassay-guided separation of the active components led to the isolation of the novel alkaloids 2(1-hydroxyethyl)-4(3H)quinazolinone (**16**) and 2-acetyl-4(3H)-quinazolinone (**17**), and the three enniatins B (**18**), B_1 (**19**) and A_1 (**20**). The structural identity of these compounds was explored extensively by 2D-NMR studies using COSY, HMQC and HMBC experiments. It is noteworthy, that the general structure of the enniatin cyclodepsipeptides has been known since the late 1940s,[19] and is characterized by alternating D-2-hydroxyisovaleric acid units (Hiv), and mixtures of N-methyl-L-valine (Me-N-Val), N-methyl-L-isoleucine (Me-N-Ile) and N-methyl-L-leucine (Me-N-Leu) units [or occasionally N-demethyl-L-amino acid units as in the case of B_2 and B_3][20] arranged in an 18-membered ring system (**Fig.4**). However, their complete

NMR data were reported only very recently; during preparation of a manuscript on our work,[21] the ^{1}H and ^{13}C NMR of enniatins A_1 and B_1 were reported by Blackwell, Miller and coworkers for the first time.[22]

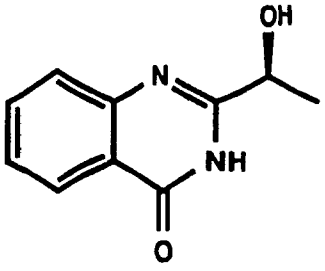

(16)

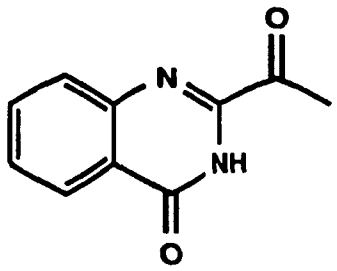

(17)

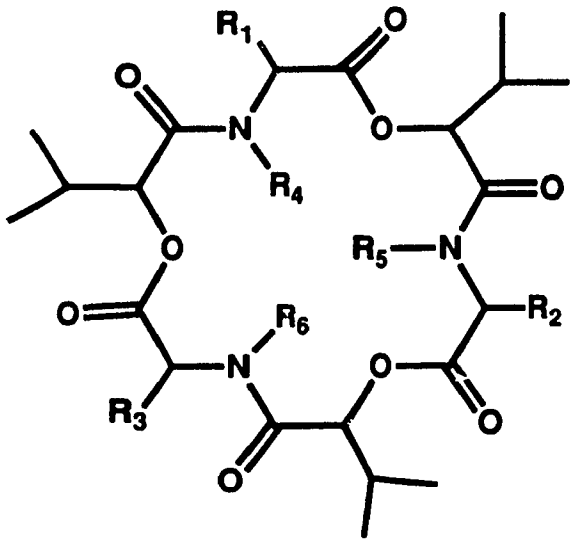

Enniatin:	R1	R2	R3	R4	R5	R6
A	*s*-Bu	*s*-Bu	*s*-Bu	Me	Me	Me
(20) A_1	*i*-pr	*s*-Bu	*s*-Bu	Me	Me	Me
(18) B	*i*-pr	*i*-pr	*i*-pr	Me	Me	Me
(19) B_1	*i*-pr	*i*-pr	*s*-Bu	Me	Me	Me
B_2	*i*-pr	*i*-pr	*i*-pr	H	Me	Me
B_3	*i*-pr	*i*-pr	*i*-pr	H	H	Me
B_4 (D)	*i*-pr	*i*-pr	*i*-Bu	Me	Me	Me
E	*i*-pr	*s*-Bu(*i*-Bu)	*i*-Bu(*s*-Bu)	Me	Me	Me
F	*i*-Bu	*s*-Bu	*s*-Bu	Me	Me	Me

Figure 4: Structures of Enniatins

2.2 Results and Discussion:

The agricultural importance of *F. lateritium* as both a biofungicide[18] and a bioherbicide,[23] has been known for some time, although investigations into the metabolites of this organism have been limited to the isolation of the antibiotic lateropyrone (**22**),[24] the mycotoxin diacetoxyscirpenol (**23**)[25] and the insecticidal cyclodepsipeptide beauvericin (**24**).[26] The production of enniatins from *F. lateritium* has also been described, however, they were isolated as a mixture and only partly identified.[21, 25]

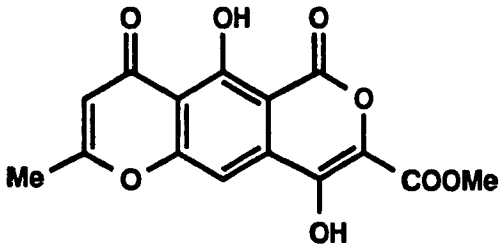

Lateropyrone (22)

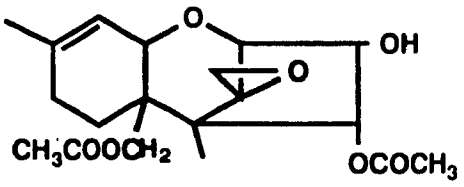

Diacetoxyscirpenol (23)

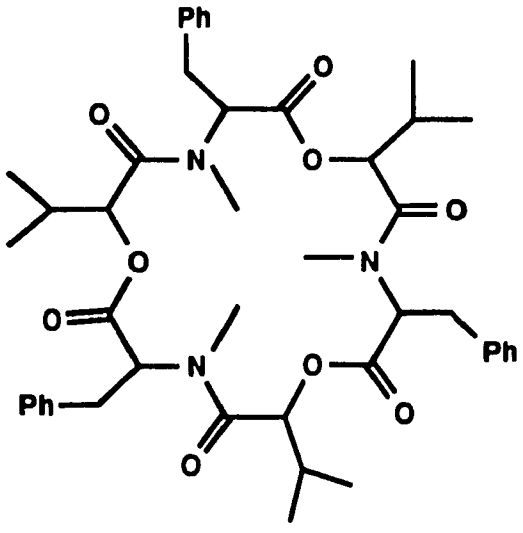

Beauvericin (24)

In this work, a bioassay-guided purification scheme was developed for the isolation of *F. lateritium* metabolites exhibiting antifungal activity against the plant pathogen *E. armeniacae*. A crude metabolite mixture of *F. lateritium* was extracted from infected solid Czapex-Dox medium with CH_2Cl_2 and partitioned by reversed phase flash column chromatography.[27] Metabolite **16** eluted from the column in 45-55% aqueous MeOH and it was isolated as an amorphous, white solid after further purification by normal phase flash column chromatography.

The ^1H NMR of **16** (**Fig.5**) (**Tab.1**, pp24) revealed the presence of a methyl group at δ 1.53 (d, 3H), coupled to an adjacent -CH-O- moiety at δ 4.73 (q, 1H). The remaining signals were assigned to four neighboring aromatic protons (δ 7.49, 7.66, 7.79 and 8.18) whose relative positions were determined by selective decoupling experiments. The ^{13}C NMR (**Fig.6**) (**Tab.1**) indicated the presence of ten non-equivalent carbon atoms, a methyl at δ 22.4, a -CH-O- at δ 68.6, three quaternary olefinic carbons at δ 122.2, 149.6 and 161.6 (two of which had to be attached to a heteroatom), four protonated aromatic carbons at δ 127.2, 127.5, 127.8 and 135.9, and an amide carbonyl at δ 164.3. Although the signal at δ 127.5 was unusually broad and of very low intensity for a protonated carbon, HMQC NMR (**Fig.7**) clearly showed its ^1J coupling to the proton at δ 7.66. This effect may be due to further long-range coupling with ^{14}N.

High resolution CI-MS of **16** gave a molecular ion at 191.08201 for the $(M^+ + 1)$ ion (calculated: 191.08205), indicating an elemental composition of $C_{10}H_{10}N_2O_2$. Its IR spectrum supported the existence of N-H, O-H, C=N and amide C=O bonds. Based on this data, as well as the long range H-C connectivity suggested by the HMBC NMR (**Fig.8**), the structure of 2(1-hydroxyethyl)-4(3H)quinazolinone was assigned to metabolite **16.**

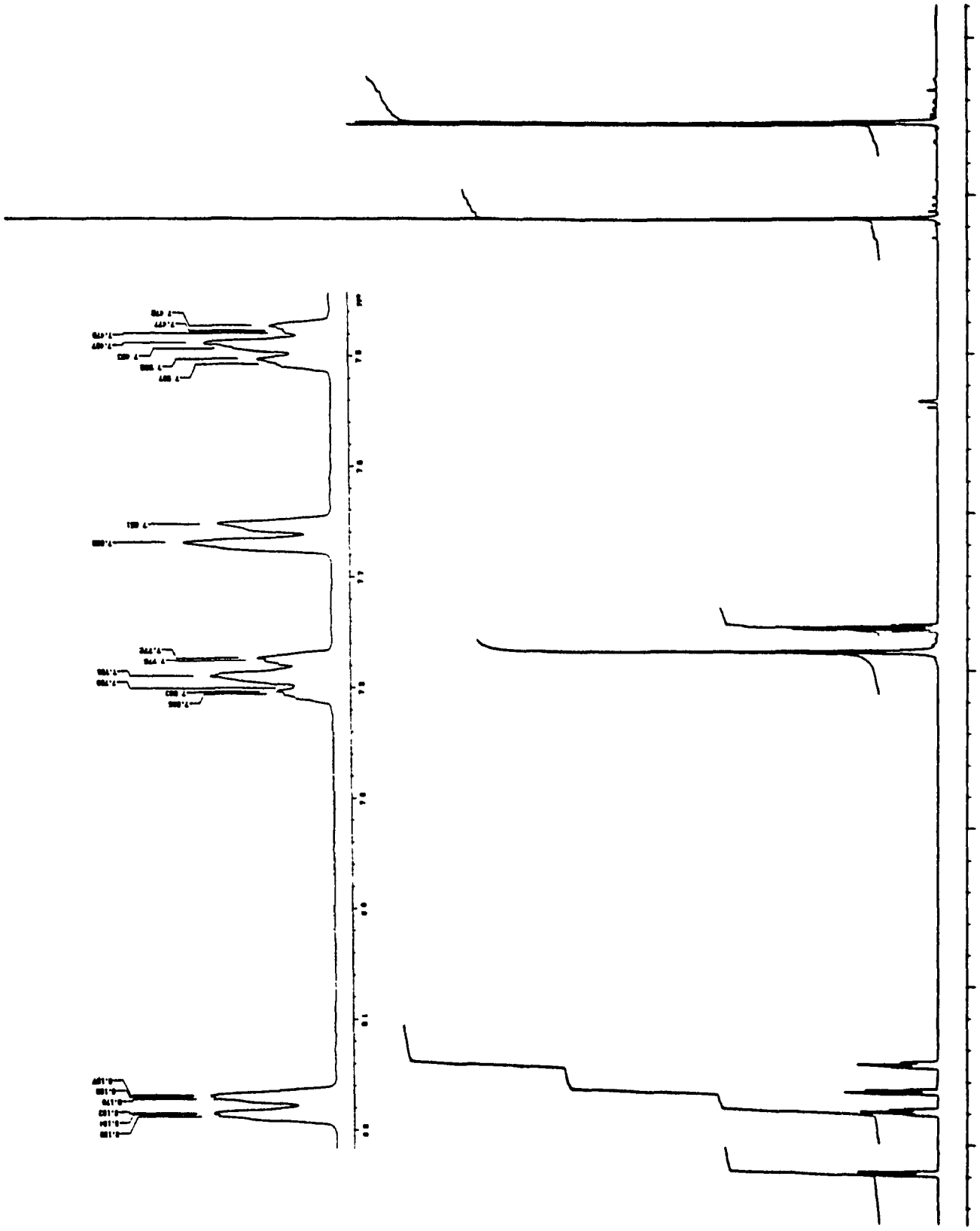

Figure 5: ^1H NMR (500 MHz, CD_3OD) of Metabolite 16

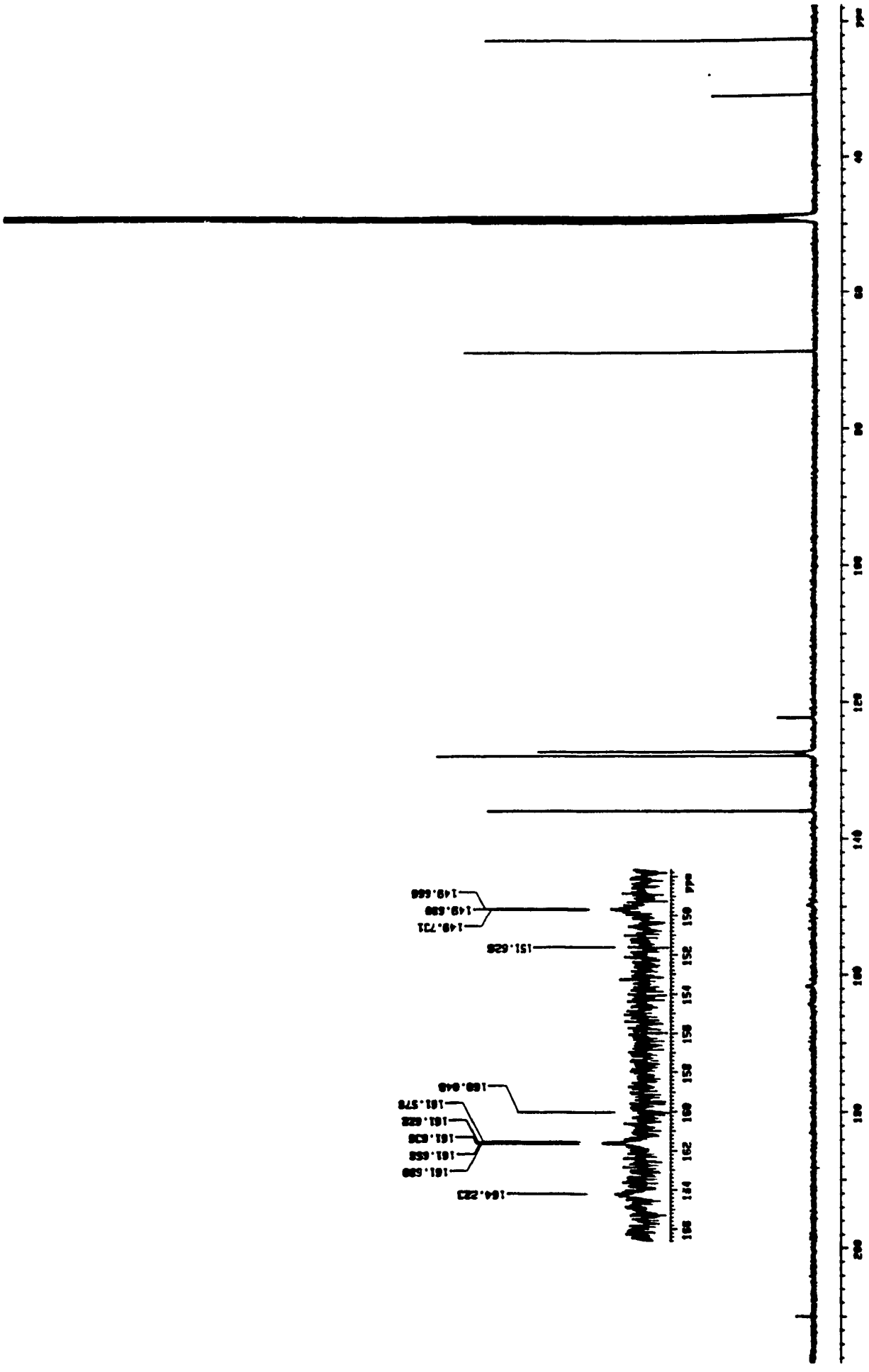

Figure 6: ^{13}C NMR (125 MHz, CD_3OD) of Metabolite 16

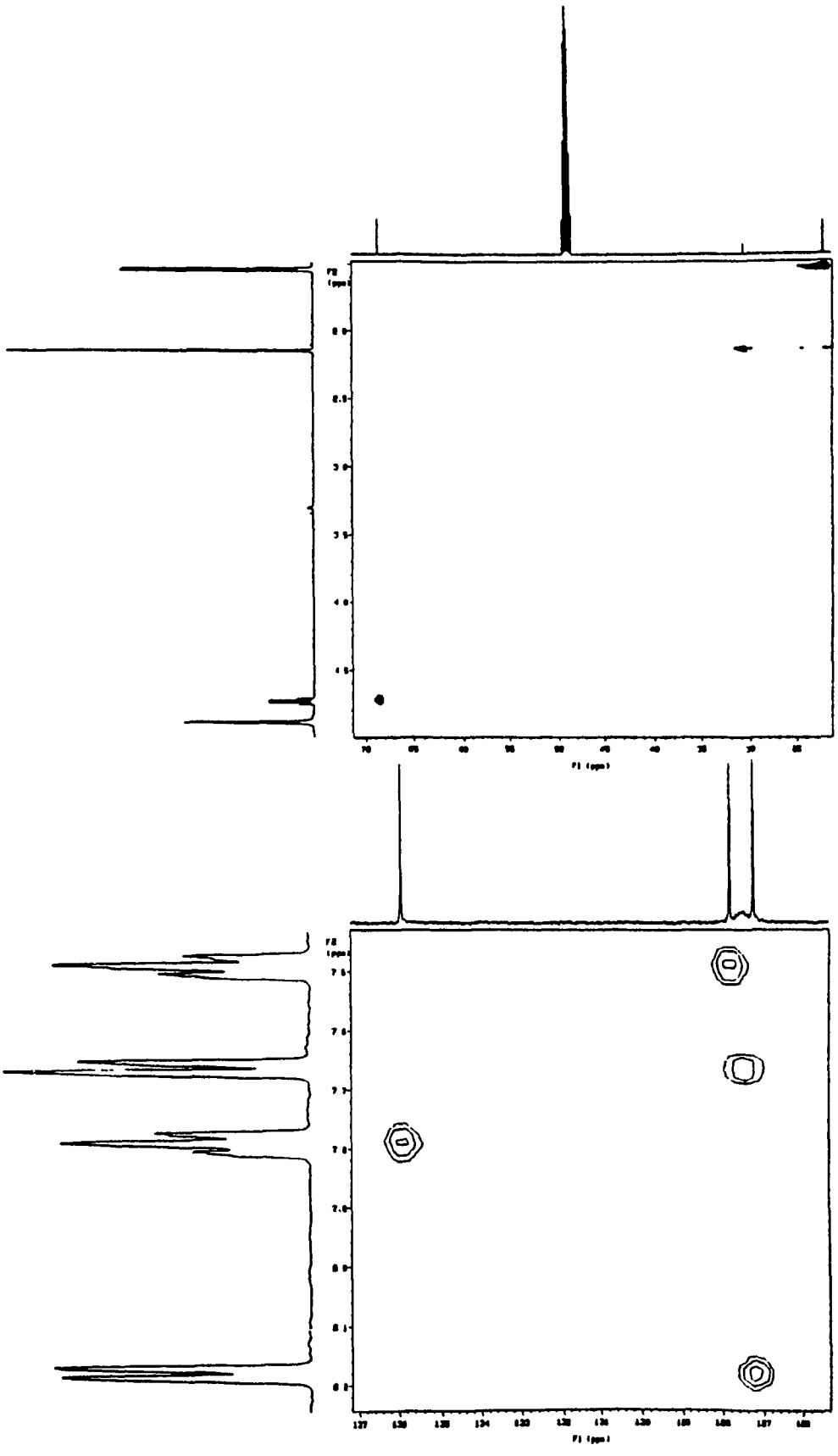

Figure 7: HMQC NMR (500 MHz, CD_3OD) of Metabolite 16

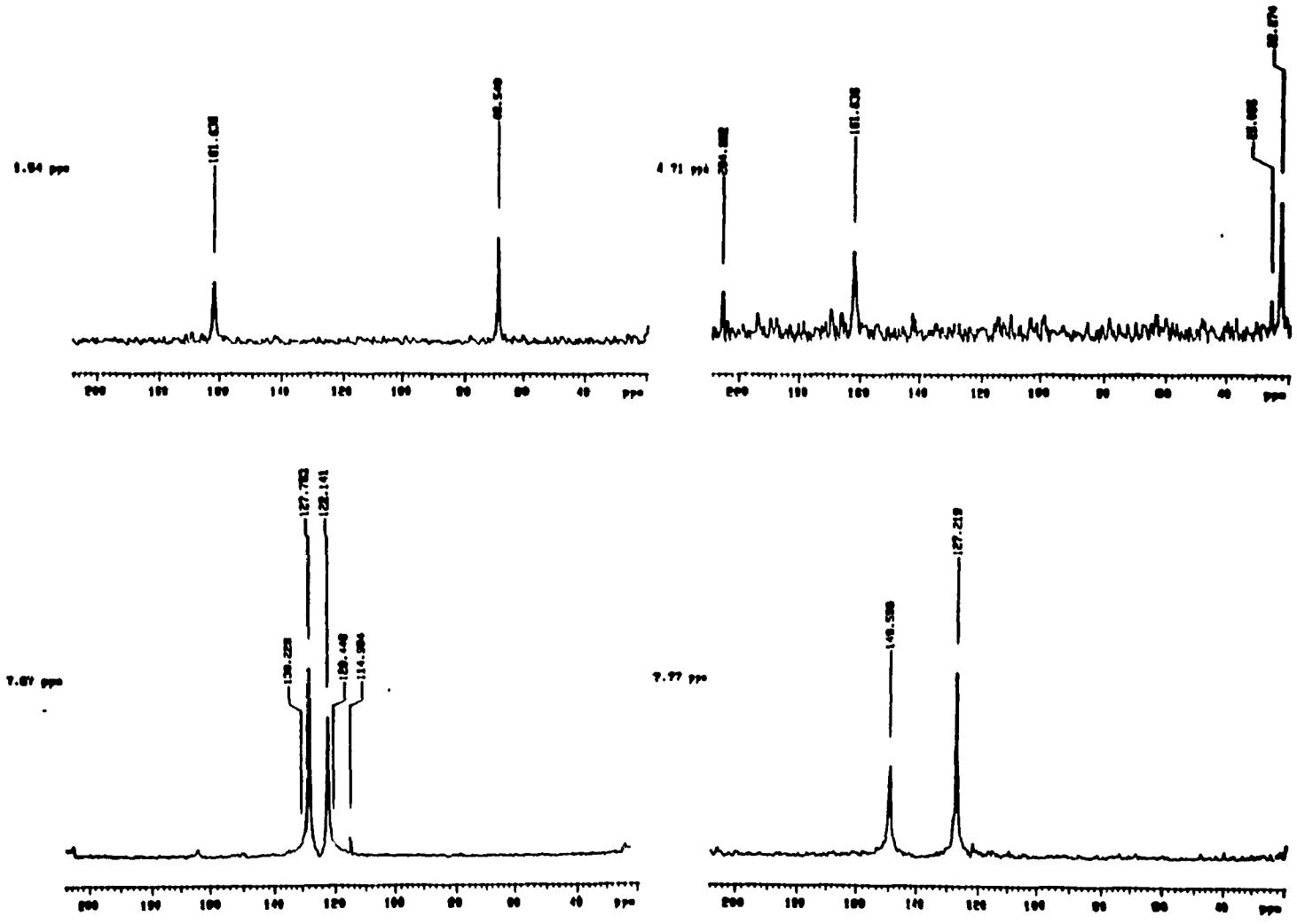

Figure 8: HMBC NMR (500 MHz, CD_3OD) of Metabolite 16

The absolute stereochemistry of **16** was investigated using Mosher's method.[28] In this technique, the absolute stereochemistry of a carbinol center, is based on the assumption that the most stable conformation of its Mosher's ester (MTPA-esters) is that which places the carbinyl proton, the ester carbonyl and the trifluoromethyl group of the MTPA moiety on the same plane.[29] Consequently, in the case of the MTPA-esters of **16**, the methyl substituent of the **S** enantiomer **[(S)-MTPA-ester of (S)-16]** will be located under the shielding effects of the phenyl group and appear upfield from the equivalent signal in the **R** enantiomer **[(S)-MTPA-ester of (R)-16]**. Using the same argument, the methoxy substituent of the MTPA moiety will be exposed to the shielding effects of the quinazolinone ring system and it should be shifted upfield in the (S)-MTPA-ester of the **S** enantiomer but not in that of the **R**.

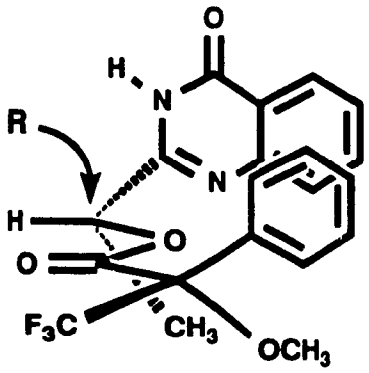

(S)-MTPA-ester of (R)-16

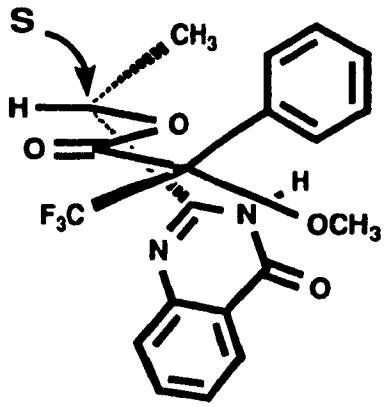

(S)-MTPA-ester of (S)-16

Fluorine NMR analysis has also been used for making stereochemical assignments of MTPA esters. The fundamental argument is again based on the preferred co-planar conformation of the trifluoromethyl group and the ester carbonyl. However, the relative extent of this preference has been shown to

depend on the magnitude of steric interactions between the phenyl group of the MTPA moiety and the adjacent carbinol substituent.[30] Therefore, it is expected that the destabilizing quinazolinone/phenyl interactions in the (S)-MTPA-ester-(**R**)-**16** will force the trifluoromethyl group away from the carbonyl deshielding plane and result in an upfield shift of the $-CF_3$ signal [relative to that of the (S)-MTPA-ester-(**S**)-**16**] in the ^{19}F NMR.

The (S)-MTPA-ester of metabolite **16** was prepared from the (R)-MTPA chloride following standard literature procedures.[28] Both the ^{1}H and ^{19}F NMRs were consistent with the presence of a diastereomeric mixture, composed of the (S)-MTPA-ester-(**R**)-**16** and the (S)-MTPA-ester-(**S**)-**16** in a ratio of ~1.5:1 (**Tab.2**). Thus, the small, negative optical rotation observed for metabolite **16** was attributed to the major **R** enantiomer. It has been speculated that the loss of optical purity is perhaps due to an equilibrium between compound **16** and its **16'** tautomer.

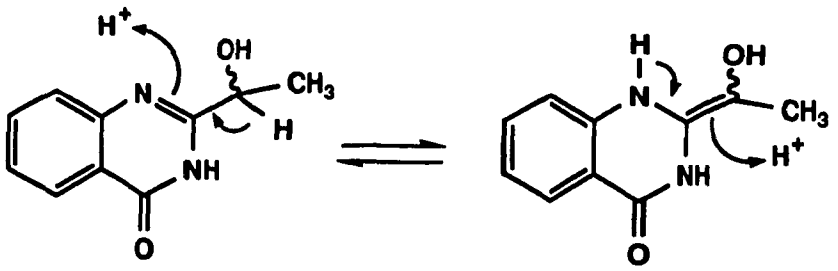

(16) **(16')**

Table 2: ^1H and ^{19}F NMR data of the (S)-MTPA-esters-16* (300MHz, $CDCl_3$)

	(S)-MTPA-ester-(R)-16		(S)-MTPA-ester-(S)-16	
	^1H (δ)	^{19}F (δ)	^1H (δ)	^{19}F (δ)
$-CH_3$	1.71 (d, J=6.6 Hz)		1.63 (d, J=6.6 Hz)	
$-OCH_3$	3.55		3.49	
-CONH-	8.9		9.2	
$-CF_3$		-71.7		-71.4

* Only the signals shown above were unambiguously assigned (due to multiple overlapping, the remaining signals in the ^1H NMR spectrum of the MTPA-sters of **16** were not assigned).

The closely related metabolite **17** was eluted from the reversed phase column in 60-70% aqueous MeOH and it was further purified by crystallization from CH_2Cl_2. Unlike the enniatin metabolites (**18**, **19** and **20**), metabolites **16** and **17** were not produced in liquid cultures of *F. lateritium* in any appreciable amounts (liquid Czapex-Dox plus 5% yeast and malt extract were tried). The ^1H NMR of **17** (**Fig.9**) (**Tab.1**) revealed the presence of an acetyl methyl at δ 2.75, four aromatic protons (δ 7.6 - 8.3) and a very broad signal at δ ~9.9 (1H). The ^{13}C NMR (**Fig.10**) was consistent with the presence of an acetate unit (C=O, δ 194.1; Me, δ 24.5) and an amide (δ 160.5), in addition to seven other aromatic or olefinic carbons; four protonated and three quaternary of which two had chemical shifts consistent with the presence of =C-N moieties (δ 147.7 and 145.3). The CI-MS data of metabolite **17** gave a molecular ion at 189

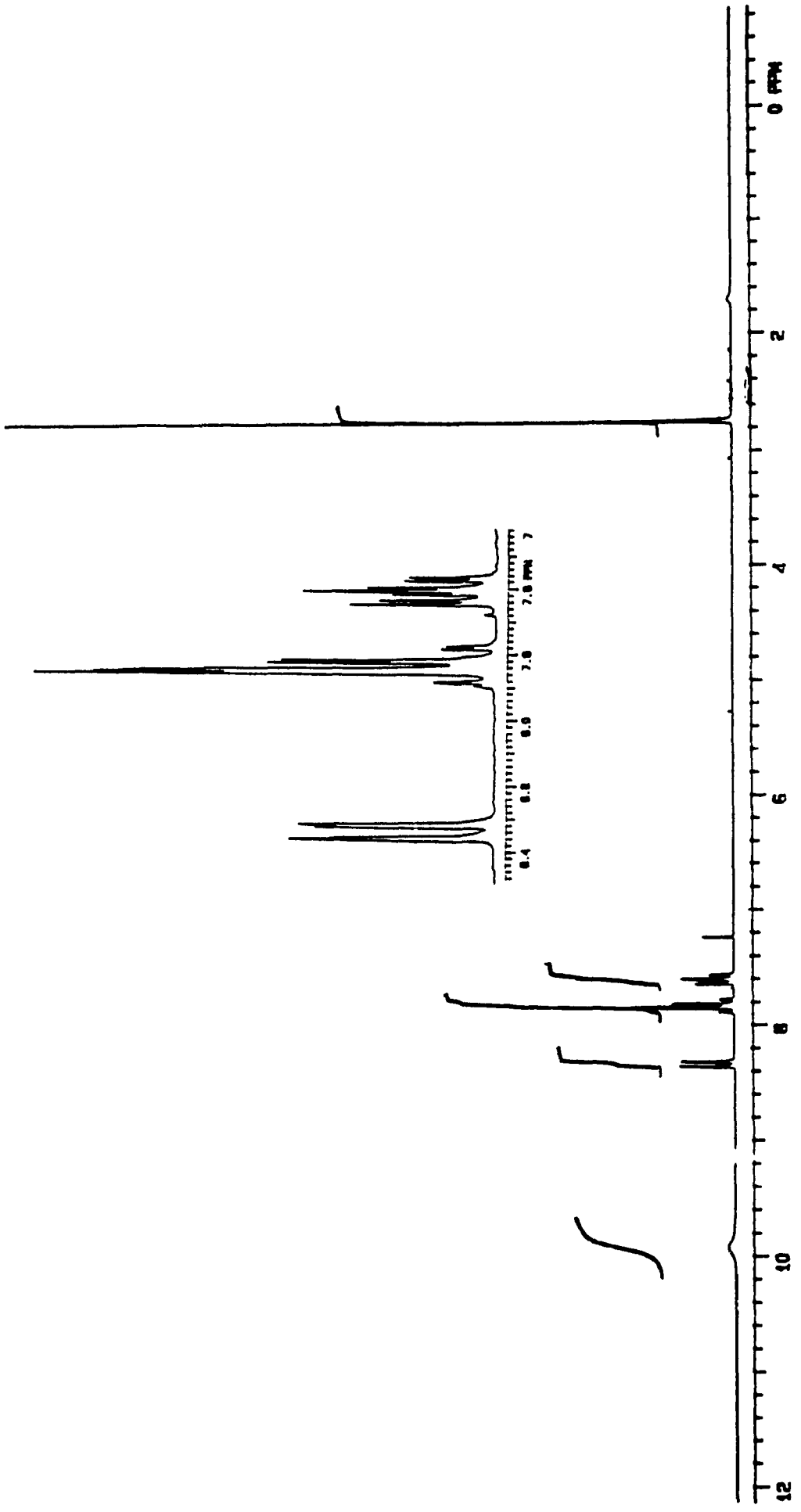

Figure 9: ^1H NMR (200 MHz, $CDCl_3$) of Metabolite 17

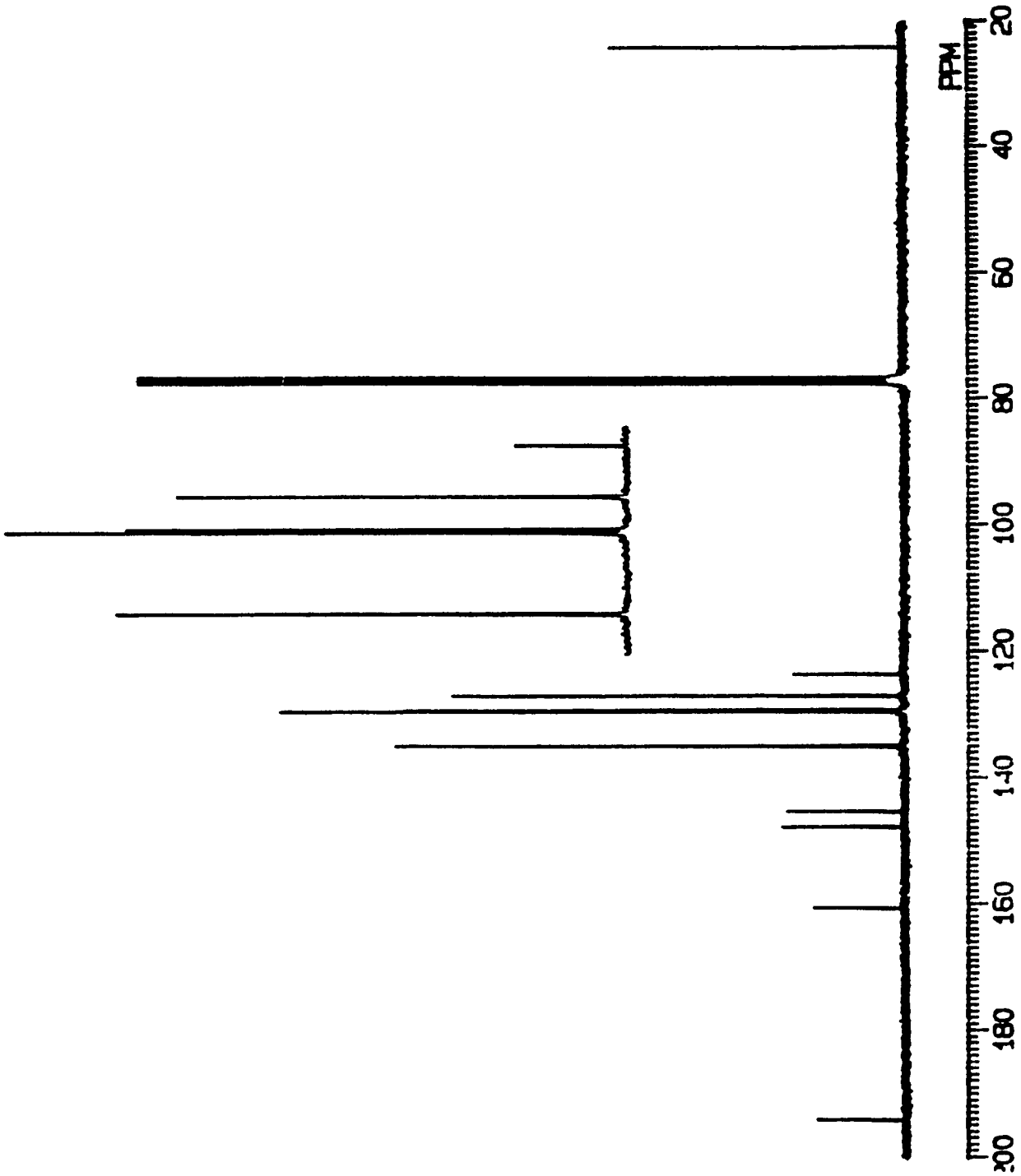

Figure 10: ^{13}C NMR (67.5 MHz, $CDCl_3$) of Metabolite 17

(M^++1) suggesting an elemental composition of $C_{10}H_8N_2O_2$ and its IR data supported the existence of N-H, N=C and C=O bonds (a strong, very broad carbonyl absorption at 1692 cm^{-1} was observed which was attributed to both an amide and a conjugated ketone). Based on this data, the structure of 2-acetyl-4(3H)quinazolinone was assigned to **17** which was later confirmed by X-ray crystallography (ORTEP diagram shown in **Fig.11**).

Table 1. ^1H and ^{13}C NMR Data of the Quinazoline Metabolites 16 and 17

	Metabolite 16 (500 MHz, CD_3OD)			Metabolite 17 (270 MHz, $CDCl_3$)	
C	**^1H (δ)**	**^{13}C(δ)**	**HMBC(δ)[b]**	**^1H(δ)**	**^{13}C(δ)**
2		161.6			147.7
NH				~9.9	
4		164.3			160.5
5		122.2			123.5
6		149.6			145.3
7	7.66	127.5[a]	122.2, 127.8	7.80[c]	129.2
8	7.79	135.9[a]	127.2, 149.6	7.80[c]	134.8
9	7.49	127.8[a]	122.2, 127.2	7.60	129.4
10	8.18	127.2[a]	135.9, 149.6	8.33	126.9
1'	4.73	68.6[a]	22.4, 161.6		194.1
2'	1.53	22.4[a]	68.6, 161.6	2.75	24.5

[a] Assignments based on the HMQC spectral data

[b] ^{13}C Shifts which are correlated to ^1H shifts in the HMBC spectra

[c] Overlapping signals in the ^1H NMR (δ 7.78-7.88).

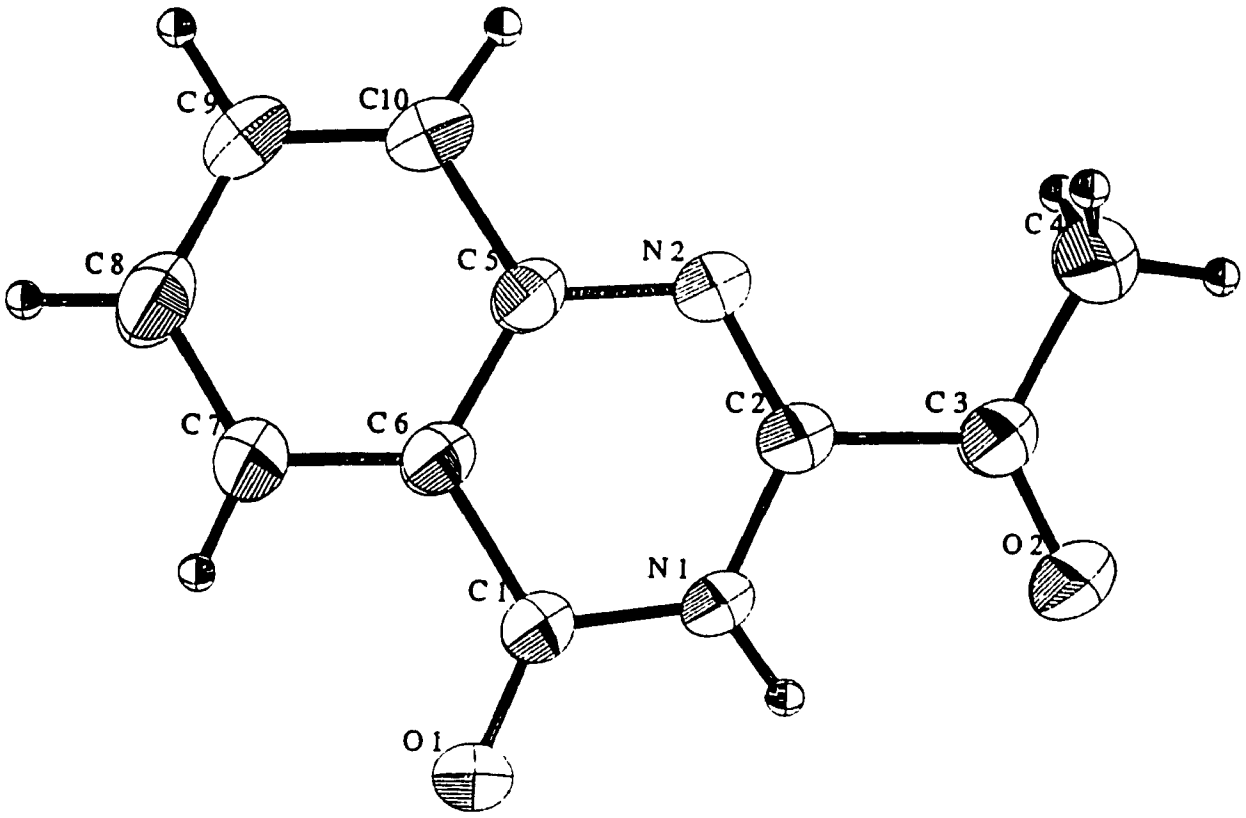

Figure 11: ORTEP Diagram of Metabolite 17

Metabolites **16** and **17** are new members of the quinazoline family of natural products (**Fig.12**). Such compounds exhibit a variety of biological properties and have been isolated from both plant and microbial sources. Among the best known examples are the plant metabolites rutaecarpine (**25**, hypotensive agent),[31] arborine (**26**, antipyretic and antihelminthic agent),[32] febrifugine (**1**) and isofebrifugine (**2**) (antimalarial),[33] and the microbial metabolites tryptanthrin (**27**, antibiotic),[34] fumiquinazolines A (**28**), B (**29**) and C (**30**) (cytotoxic agents).[35]

Figure 12: Quinazoline Natural Products

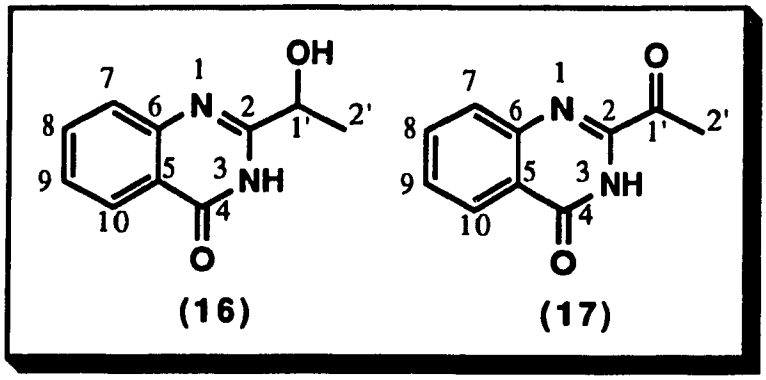

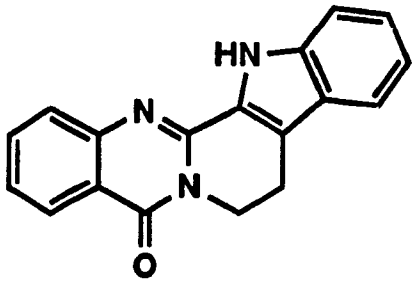

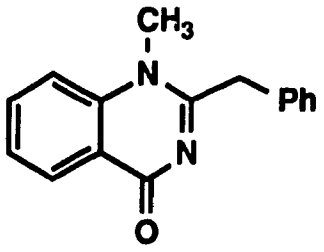

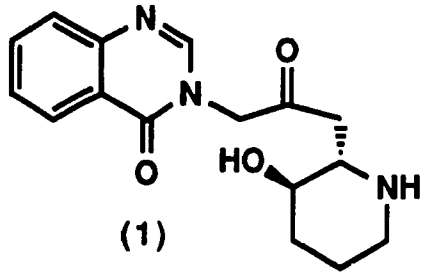

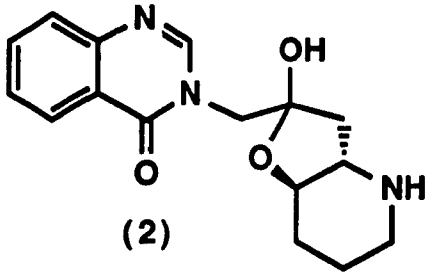

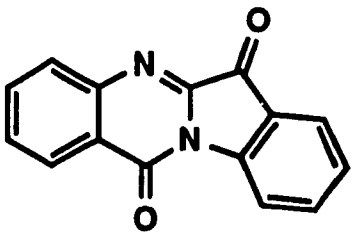

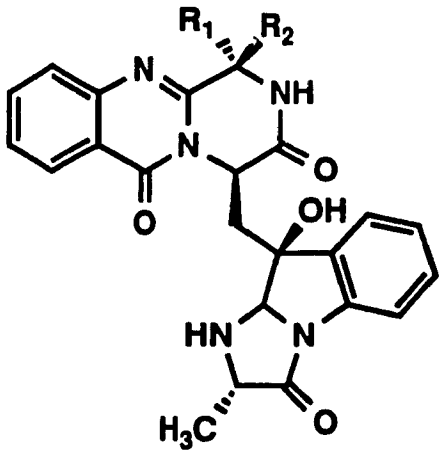

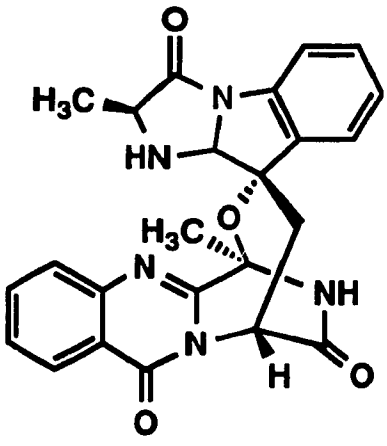

The enniatin metabolites **18**, **19** and **20** were first eluted from the reversed flash column as a mixture (with 80-100% aqueous MeOH) and subsequently purified by semi-preparative HPLC. FAB MS showed the characteristic molecular ions of enniatins B (**18**), B_1 (**19**) and A_1 (**20**), along with several metal complex ions (Na^+, K^+ and Cs^+) indicative of the ionophoric properties of these compounds.[36]

All of the IR and NMR data of metabolites **18**, **19** and **20** were consistent with their identification as the enniatins B, B_1 and A_1 respectively.[37,22] For example, the high degree of symmetry in the molecular structure of enniatin B was clearly evident in both its ^1H and ^{13}C NMR data (**Fig.13** and **14** respectively); even at high magnetic field (500 MHz for ^1H) only one set of signals was observed for all three N-Me-valine--hydroxyisovaleric acid units (**Tab.3**). All of the 2D-NMR data of metabolite **18** [COSY (**Fig.15**), HMQC (**Fig.16**) & HMBC (**Fig.17**); **Tab.3**] and the previous reported ^{13}C NMR of enniatin B [21] were consistent with its identification as enniatin B.

Table 3: ^{1}H and ^{13}C NMR Data of Enniatin B (18) (500MHz, $CDCl_3$)

Carbon	$^{1}H(\delta)$	$^{13}C(\delta)$	COSY(δ)	HMBC(δ)[b]
N-Me-Val				
-C=O		169.1		
α-CH	4.51	63.0[a]	2.29	170.1, 169.1, 33.1, 27.7 20.2
β-CH	2.29	27.7[a]	4.51, 0.88, 1.05	170.1, 63.0, 20.2, 19.1
γ-CH_3	1.05	20.2[a]	2.29	63.0, 27.7, 19.1
γ-CH_3	0.88	19.1[a]	2.29	63.0, 27.7, 20.2
N-CH_3	3.12	33.1[a]	_	169.1, 63.0
Hiv				
-C=O		170.1		
α-CH	5.13	75.5[a]	2.26	170.1, 29.7, 18.5, 18.3[c]
β-CH	2.26	29.7[a]	5.13, 0.97, 0.95	75.5, 18.5, 18.3[c]
γ-CH_3	0.97	18.5[a]	2.26	75.5, 29.7, 18.3[c]
γ-CH_3	0.95	18.3[a]	2.26	75.5, 29.7, 18.5[c]

[a] Assignments based on the HMQC spectral data

[b] ^{13}C Shifts which are correlated to ^{1}H shifts in the HMBC spectra

[c] Due to the small $\Delta\delta$ of the γ-Me signals in the ^{13}C NMR, their identity in the HMBC isn't clear.

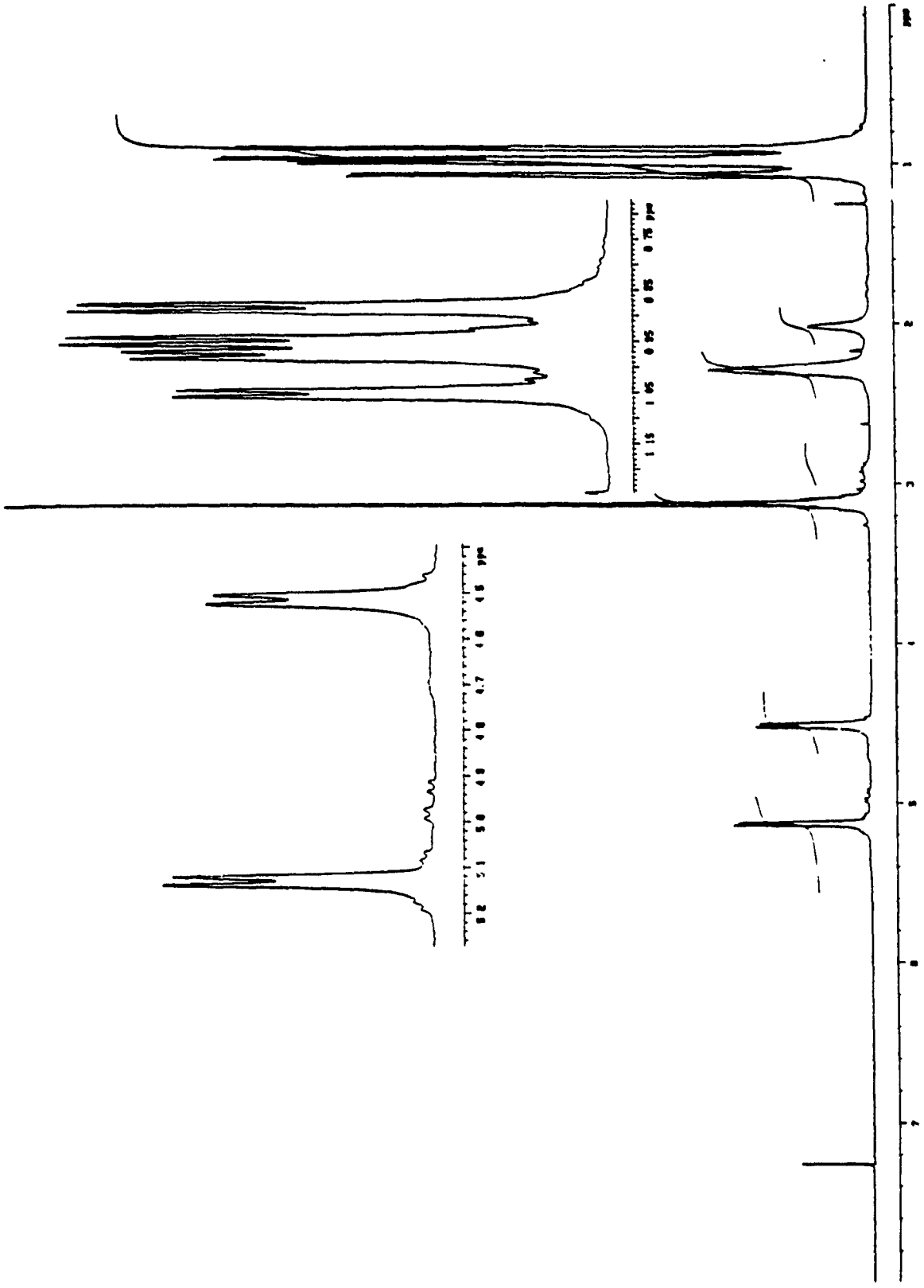

Figure 13: ^1H NMR (500 MHz, $CDCl_3$) of Metabolite 18

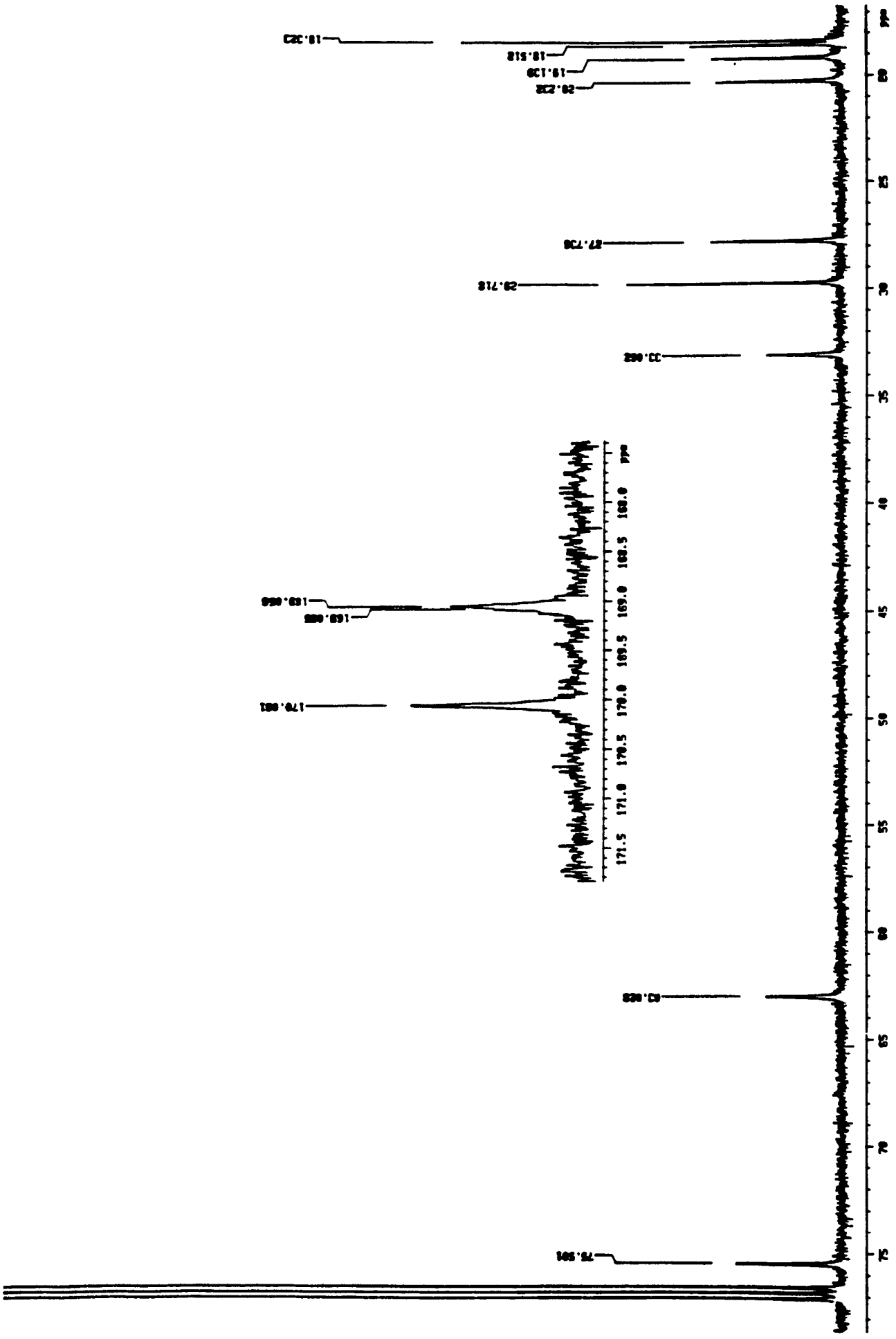

Figure 14: ^{13}C NMR (125 MHz, $CDCl_3$) of Metabolite 18

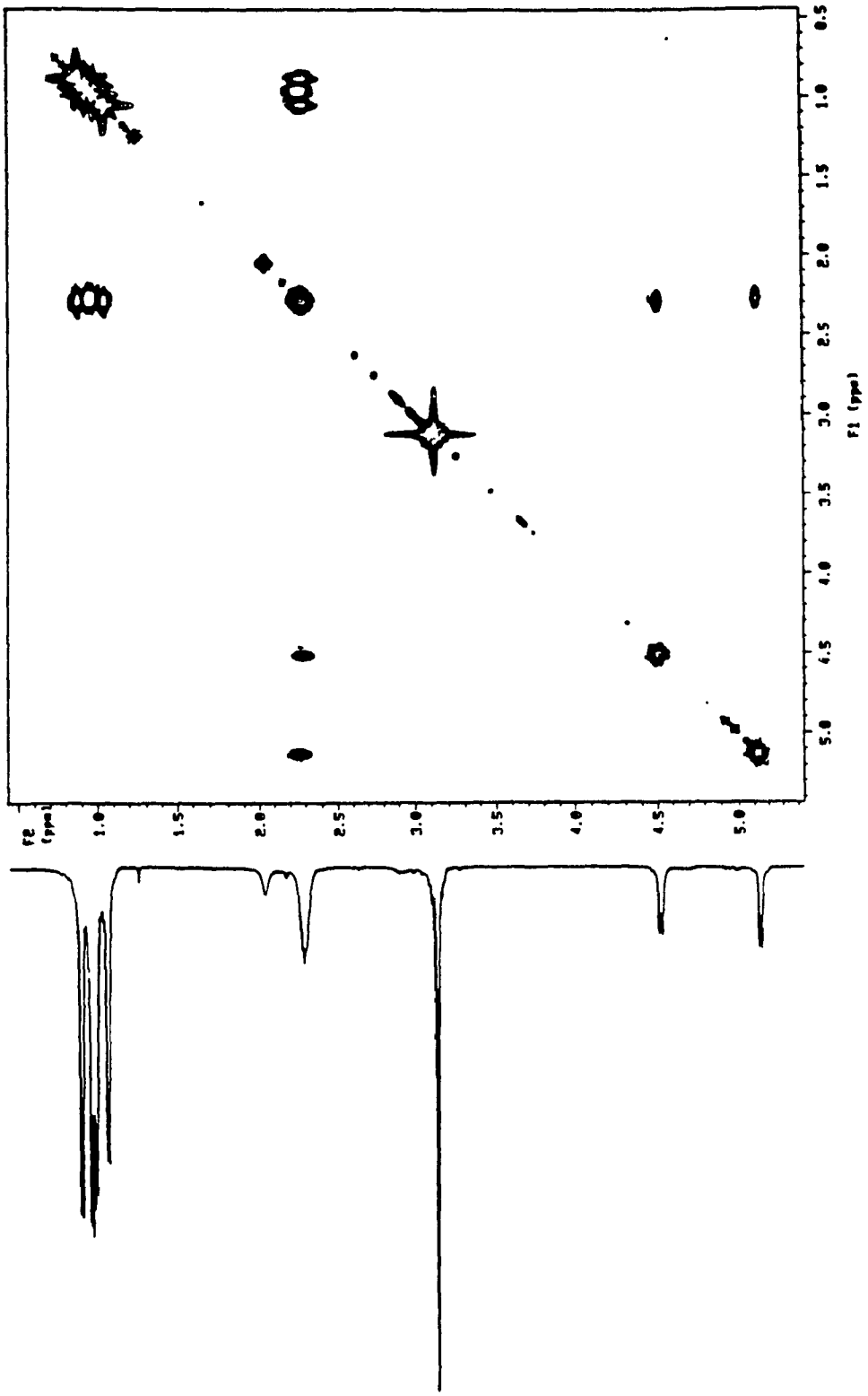

Figure 15: COSY NMR (500 MHz, $CDCl_3$) of Metabolite 18

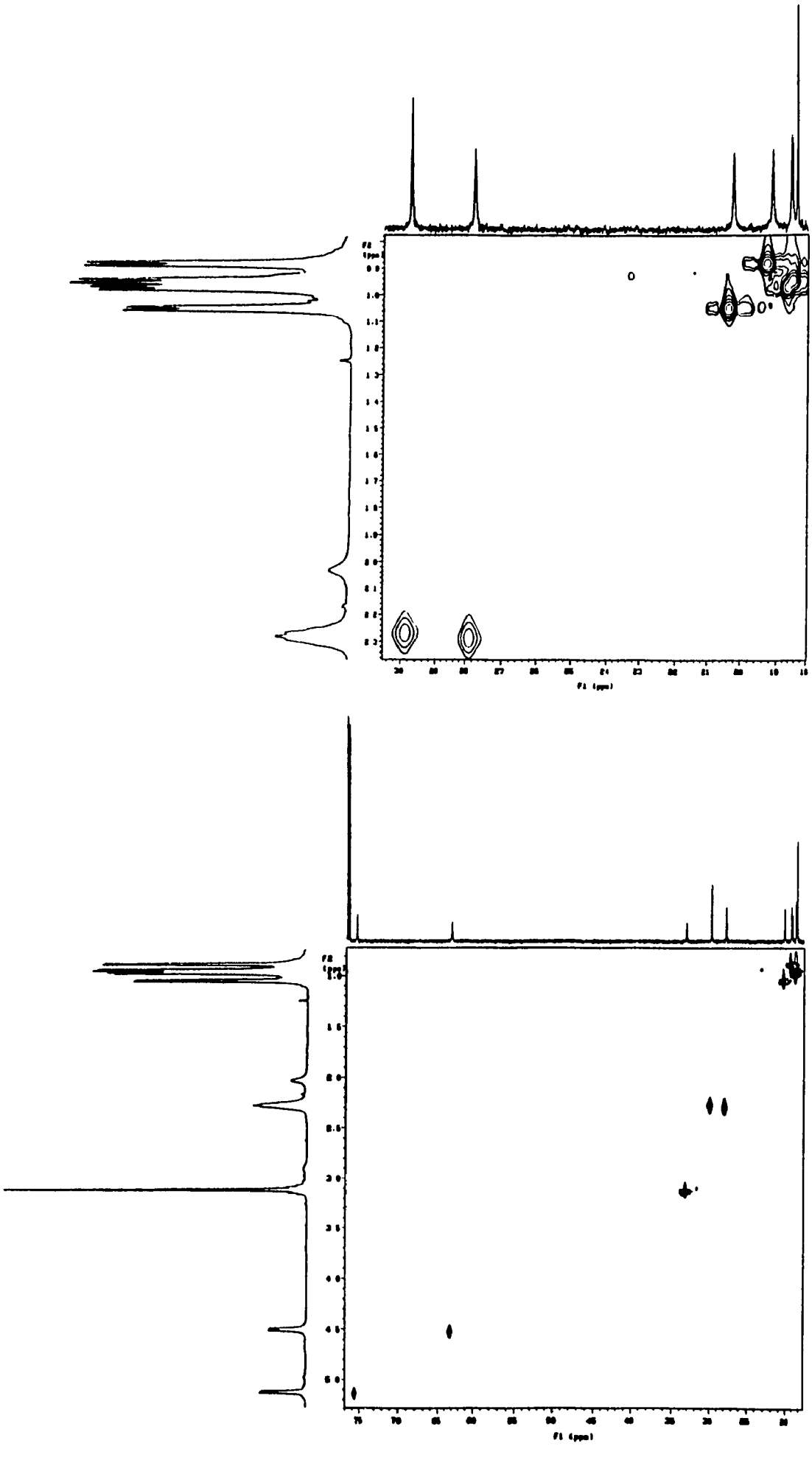

Figure 16: HMQC NMR (500 MHz, $CDCl_3$) of Metabolite 18

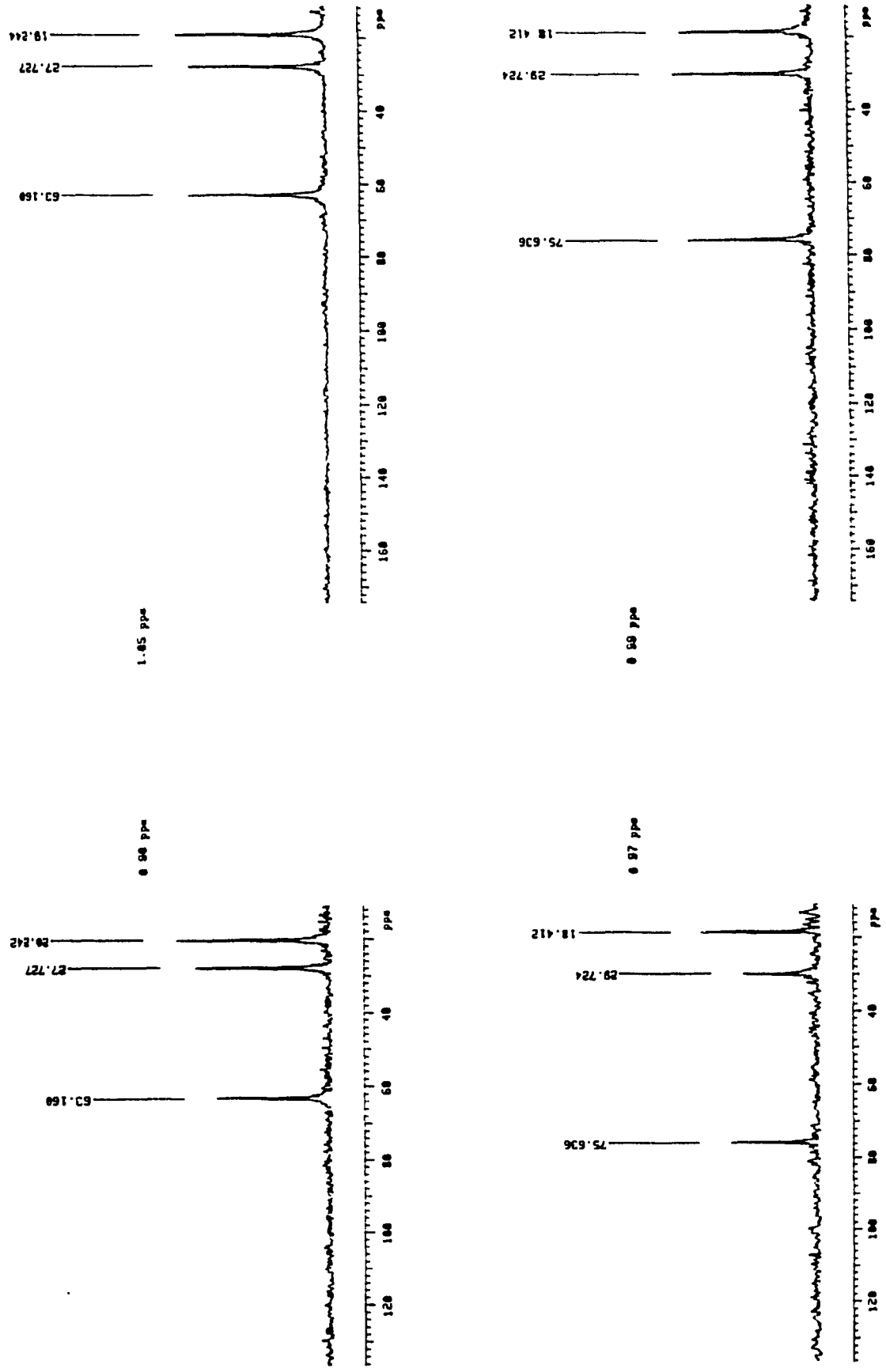

Figure 17: HMBC NMR (500 MHz, $CDCl_3$) of Metabolite 18

Structure elucidation and assignment of all ^{1}H and ^{13}C NMR signals of metabolites **19** (**Fig.18** and **Fig.19** respectively) and **20** (**Fig.22** and **Fig.23** respectively) was achieved from the combined COSY (**Fig.20** and **Fig.24** for metabolites **19** and **20** respectively), HMQC (**Fig.21** and **Fig.25** for metabolites **19** and **20** respectively) and HMBC (**Tab.4** for metabolite **19**) NMR data. The data obtained was completely consistent with that recently reported and it is summarized in **Tab.4** and **Tab.5**.[22]

Table 4: ^{1}H and ^{13}C NMR Data of Enniatin B_1 (19) (500MHz, $CDCl_3$)

Carbon	$^{1}H(\delta)$	$^{13}C(\delta)$	COSY(δ)	HMBC(δ)
N-Me-Val				
-C=O		169.0		
α-CH	4.50	63.1[a]	2.30	170.1, 169.0, 33.2, 27.9, 20.3, 19.2
α-CH	4.45	63.3[a]	2.30	170.1, 169.0, 33.3, 27.8, 19.2
β-CH	2.30	27.8, 27.9[a]	4.50, 4.45, 1.05, 0.88	170.1, 63.3, 63.1, 20.3, 19.2
γ-CH_3	1.05	20.3[a]	2.30	63.3, 63.1, 27.8, 19.2
γ-CH_3	0.88	19.2[a]	2.30	63.3, 63.1, 27.8, 20.3
N-CH_3	3.12	33.2, 33.3[a]	_	169.0, 63.3
N-Me-Ile				
-C=O		169.0		
α-CH	4.72	61.2[a]	2.07	170.2, 169.0, 33.7, 32.5, 25.1, 16.0
β-CH	2.07	33.7[a]	4.72, 1.41, 0.99	16.0
γ-CH_2	1.41	25.1[a]	2.07, 1.10, 0.86	
	1.10	25.1[a]	1.41, 0.86	16.0
γ-CH_3	0.99	16.0[a]	2.07	61.2, 33.7, 25.1
δ-CH_3	0.86	10.7[a]	1.41, 1.10	33.7, 25.1
N-CH_3	3.10	32.5[a]	_	169.0, 61.2
Hiv				
-C=O		170.2, 170.1		
α-CH	5.15	75.2[a]	2.27	170.1, 29.7, 18.4[c]
α-CH	5.12	75.6[a]	2.27	170.1, 169.0, 29.7,18.5[c]
α-CH	5.09	75.6[a]	2.27	
β-CH	2.27	29.7[a]	5.15, 5.12, 5.09, 0.93-0.99	169.0, 75.6, 75.2, 18.4[c]
γ-CH_3	0.93-0.99[b]	18.2-18.5[a,b]	2.27	75.6, 75.2, 29.7, 18.2[c], 18.5[c]

[a] Assignments based on the HMQC spectra [b] Multiple overlapping signals
[c] One of the γ-Me which can't tell exactly

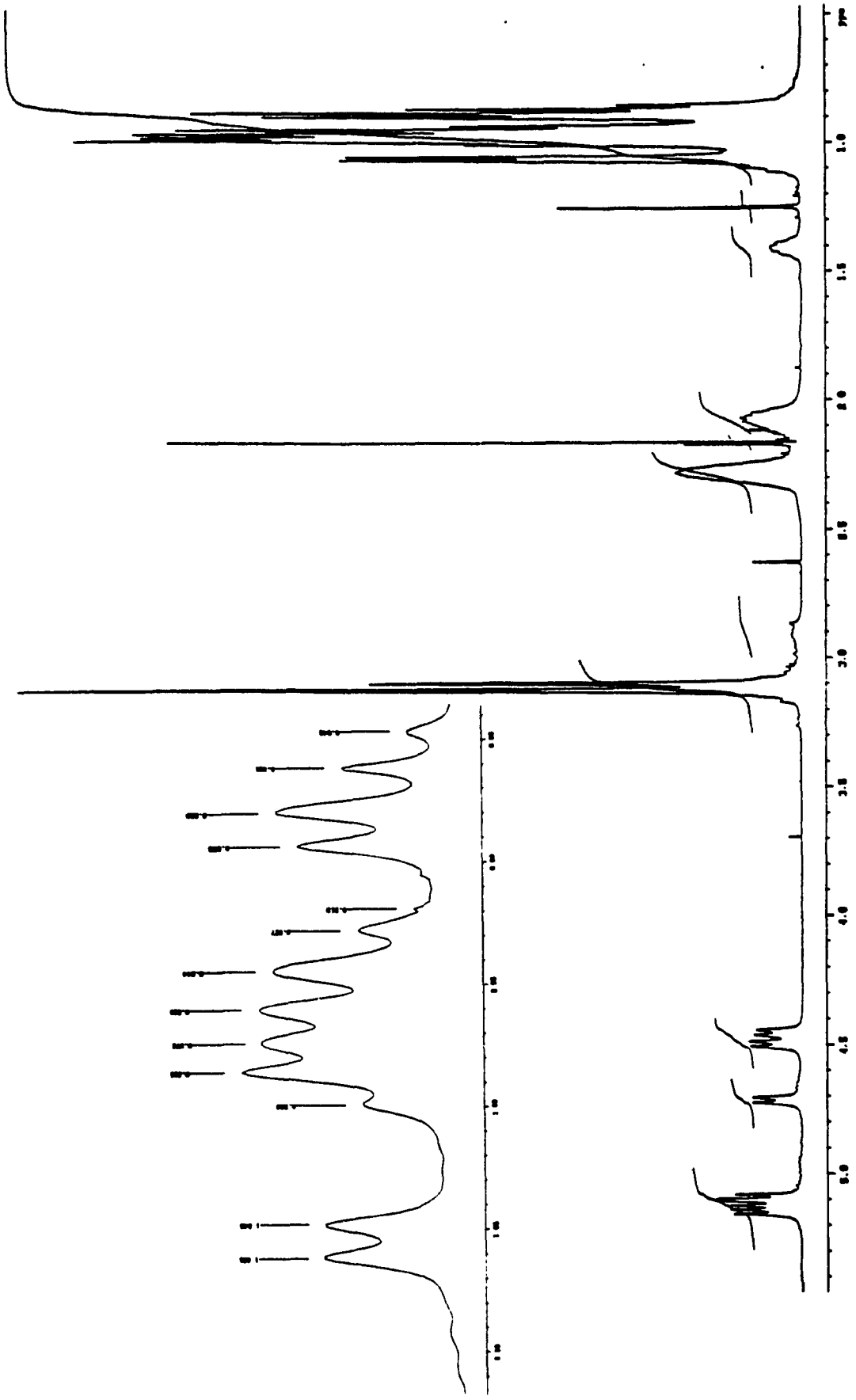

Figure 18: ^{1}H NMR (500 MHz, $CDCl_3$) of Metabolite 19

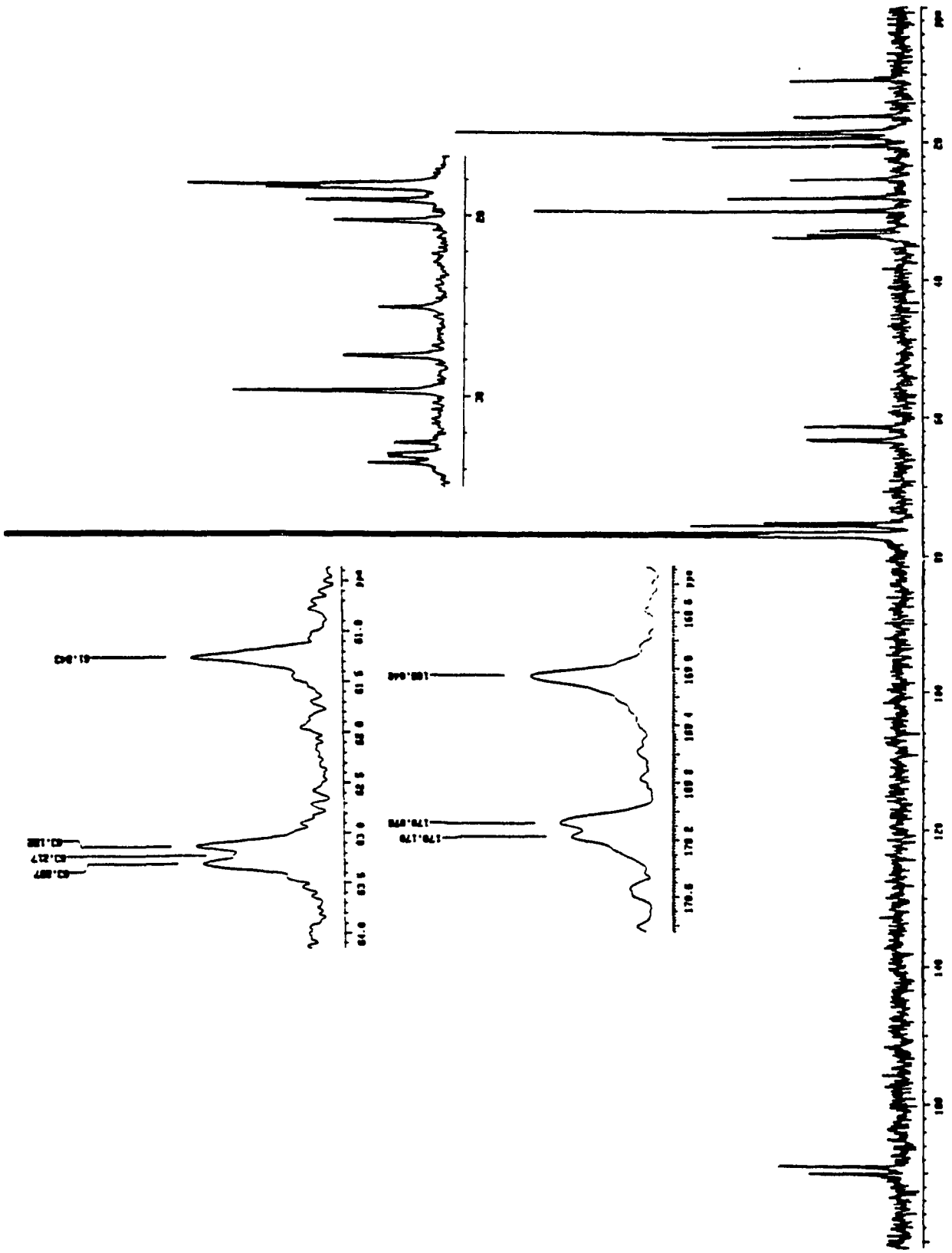

Figure 19: ^{13}C NMR (125 MHz, $CDCl_3$) of Metabolite 19

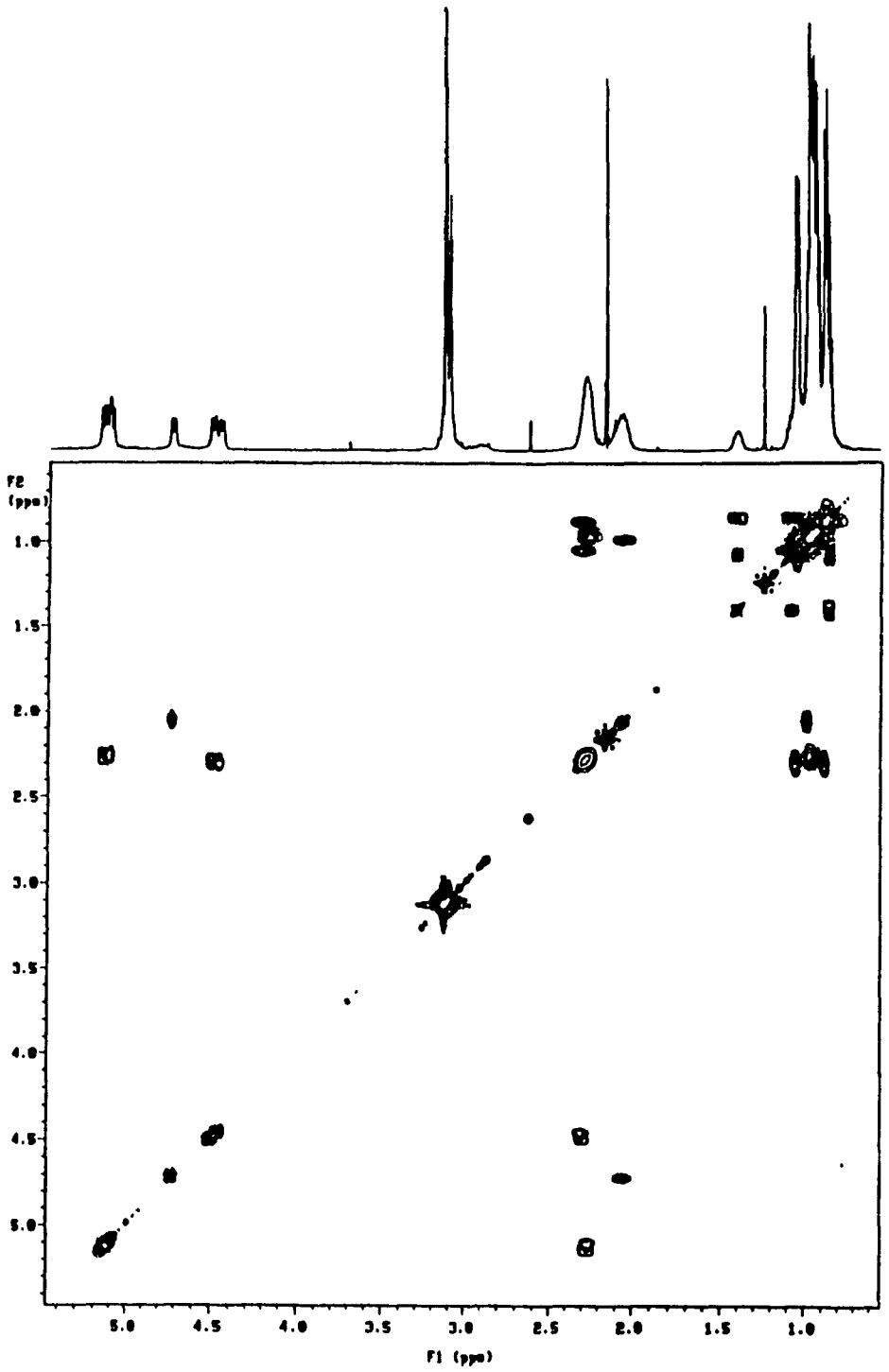

Figure 20: COSY NMR (500 MHz, $CDCl_3$) of Metabolite 19

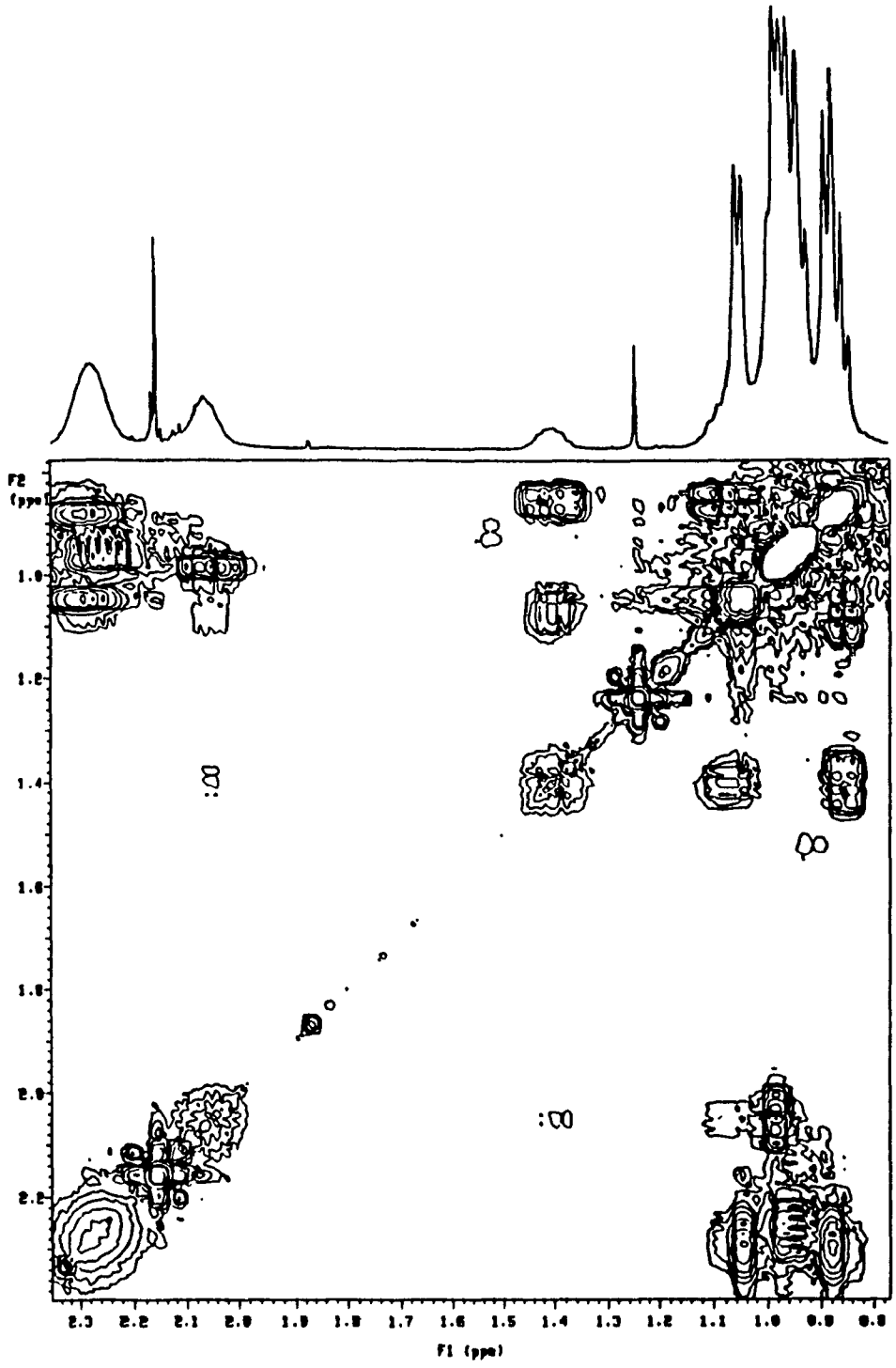

Figure 20: COSY NMR (500 MHz, $CDCl_3$) of Metabolite 19

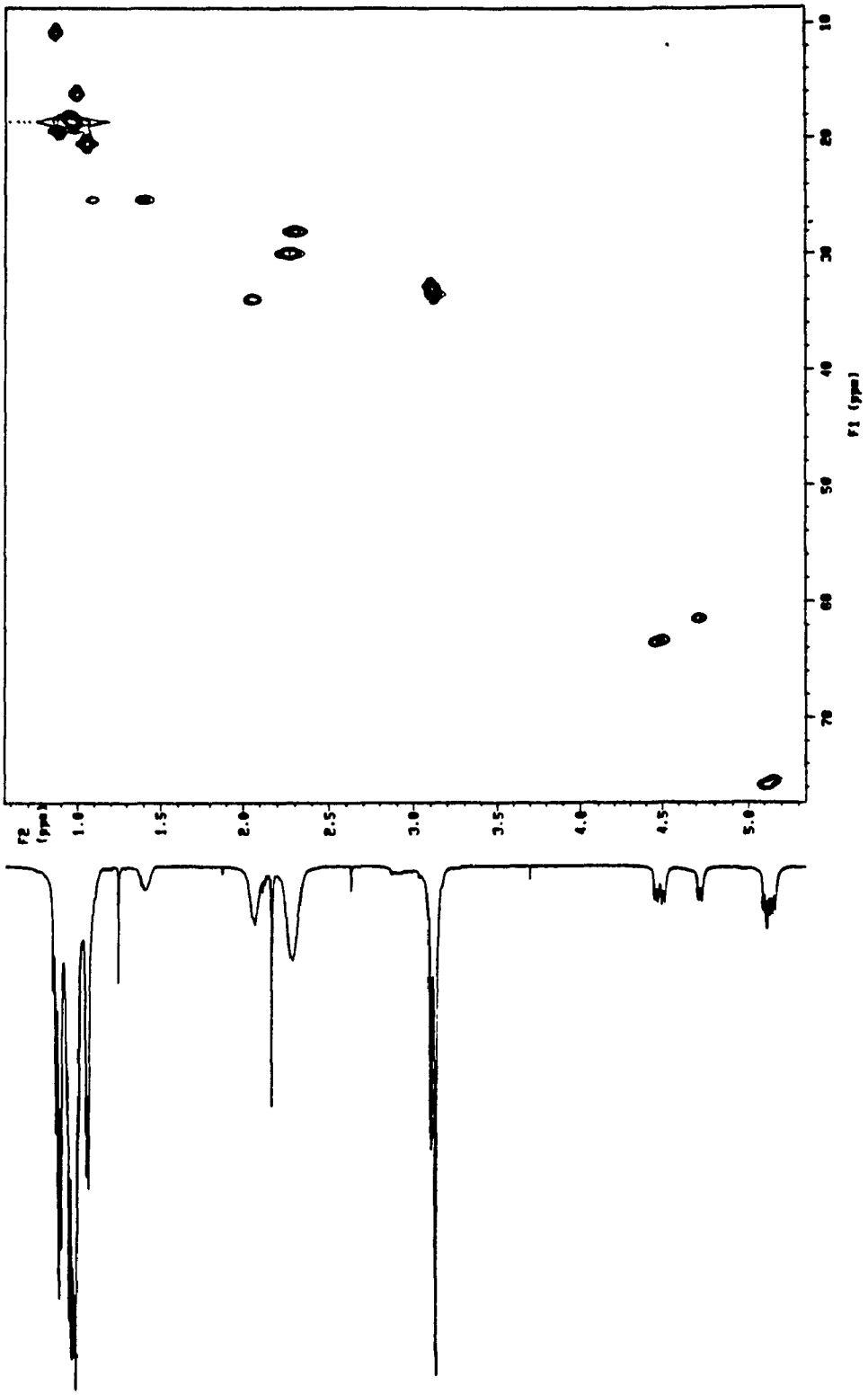

Figure 21: HMQC NMR (500 MHz, $CDCl_3$) of Metabolite 19

Table 5: ^{1}H and ^{13}C NMR Data of Enniatin A_1 (500MHz, $CDCl_3$)

Carbon	$^{1}H(\delta)$	$^{13}C(\delta)$	COSY(δ)
N-Me-Val			
-C=O		169.1	
α-CH	4.45	63.4[a]	2.31
β-CH	2.31	27.9[a]	4.45, 1.07, 0.90
γ-CH_3	1.07	20.4[a]	2.31
γ-CH_3	0.90	19.3[a]	2.31
N-CH_3	3.14	33.4[a]	–
N-Me-Ile			
-C=O		169.1	
α-CH	4.71	61.4[a]	2.06
	4.69	61.5[a]	2.06
β-CH	2.06	33.7, 33.8[a]	4.70, 1.41, 1.00
γ-CH_2	1.41	25.2[a]	2.06, 1.08, 0.86
	1.08	25.2[a]	1.41, 0.86
γ-CH_3	1.00	16.0[a]	2.06
δ-CH_3	0.86	10.7[a]	1.41, 1.08
N-CH_3	3.11	32.6[a]	–
Hiv			
-C=O		170.2, 170.1	
α-CH	5.15	75.3[a]	2.26
α-CH	5.12	75.3[a]	2.26
α-CH	5.09	75.8[a]	2.26
β-CH	2.26	29.7[a]	5.15, 5.12, 5.09, 0.94-1.00
γ-CH_3	0.94-1.00[b]	18.3-18.5[a,b]	2.26

[a] Assignments based on the HMQC spectra

[b] Multiple overlapping signals

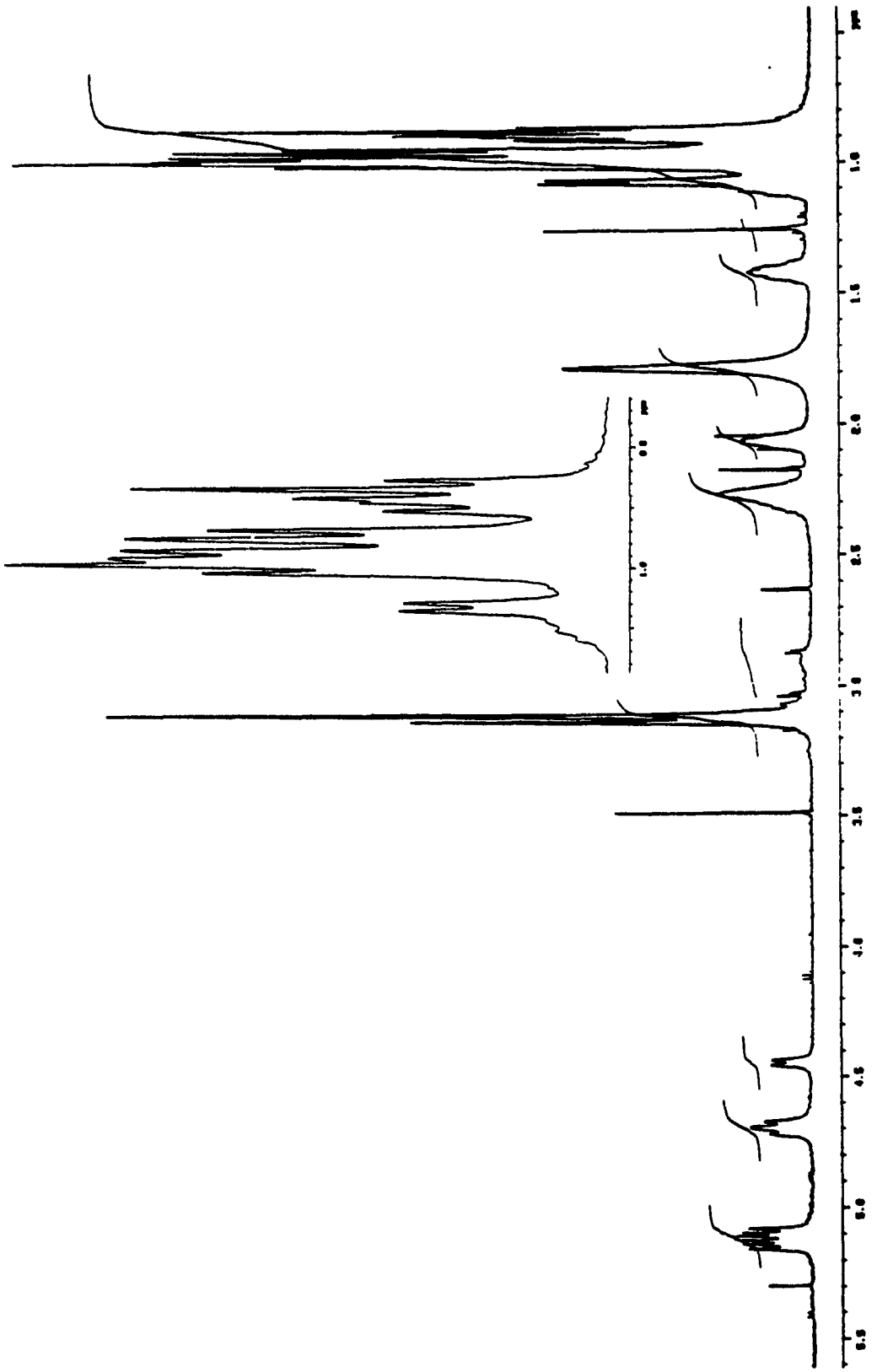

Figure 22: ^1H NMR (500 MHz, $CDCl_3$) of Metabolite 20

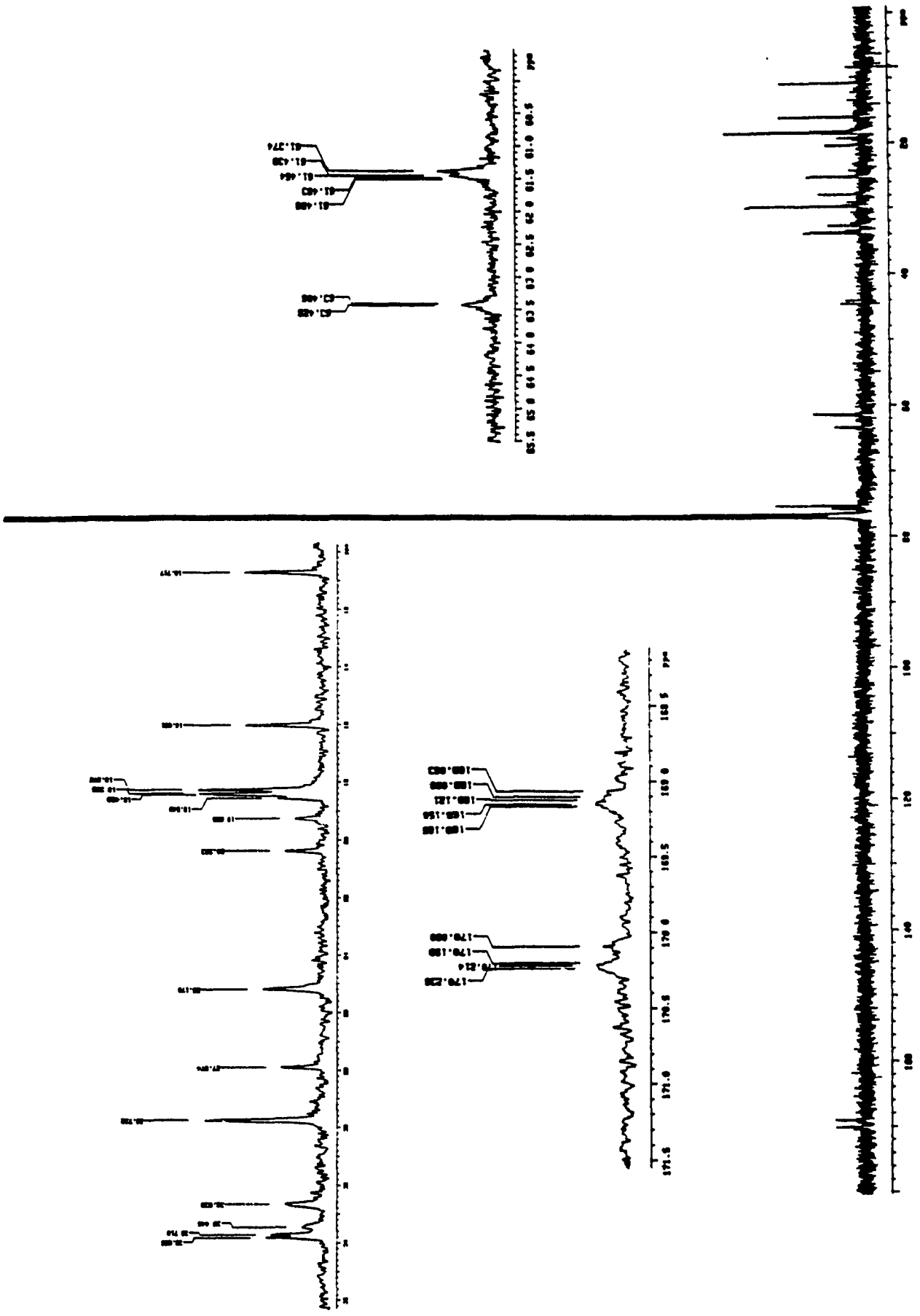

Figure 23: ^{13}C NMR (125 MHz, $CDCl_3$) of Metabolite 20

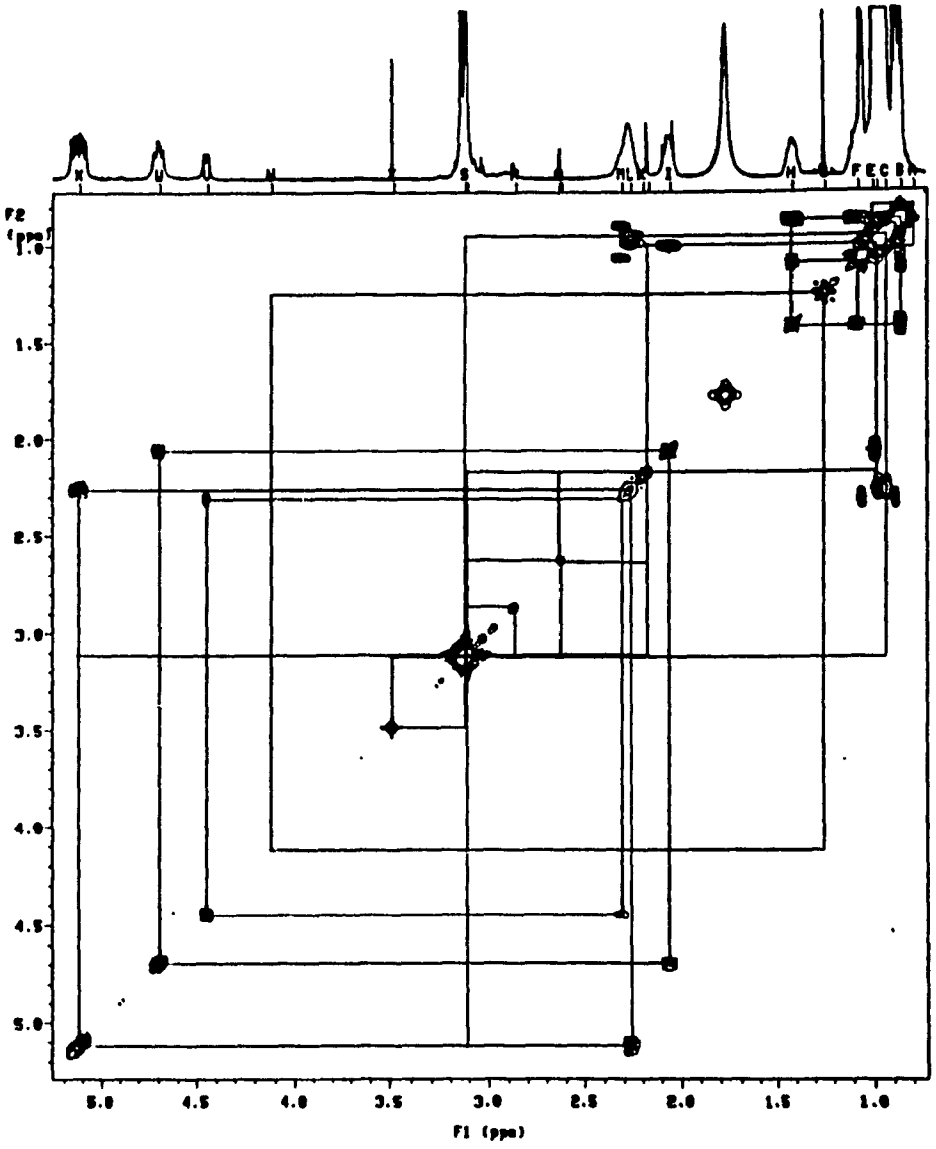

Figure 24: COSY NMR (500 MHz, $CDCl_3$) of Metabolite 20

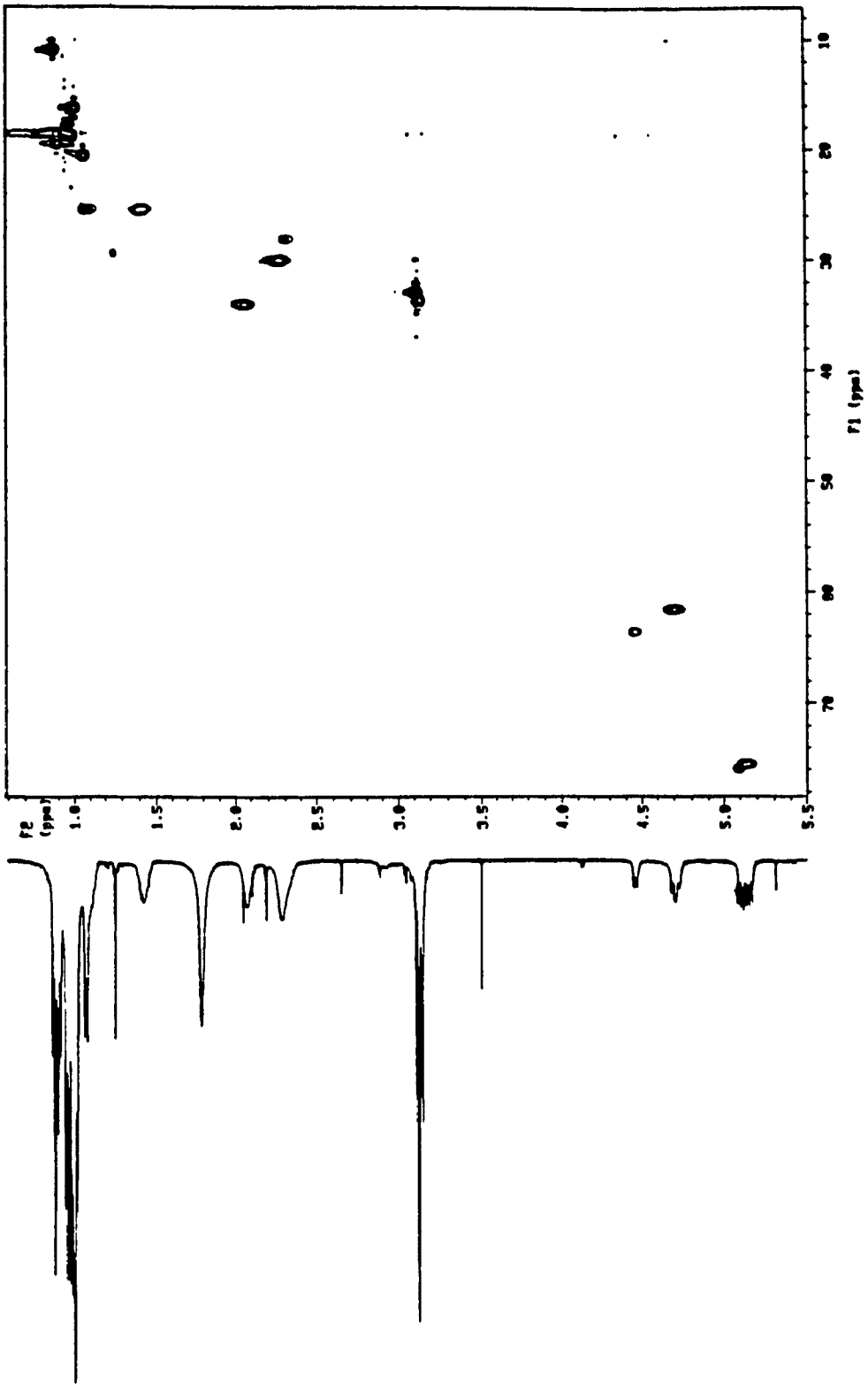

Figure 25: HMQC NMR (500 MHz, $CDCl_3$) of Metabolite 20

The enniatin metabolites are knowr. to exhibit insecticidal[38,39] antibiotic[40] and phytotoxic activities,[41] and to also inhibit cholesterol biosynthesis.[42] In this work, the antagonistic effect of *F. lateritium* against the important plant pathogen *E. armeniacae* was investigated. Potent antifungal activity against *E. armeniacae* was observed with metabolites **18**, **19** and **20**. Therefore, it appears that the production of enniatins B (**18**), B_1 (**19**) and A_1 (**20**) by *F. lateritium* may play a key role in the biological effects of this organism as a biofungicide.[17]

As part of a broader biological screening of microbial metabolites, some of the compounds presented in this paper were evaluated for their ability to inhibit HIV replication in C8166 cells [as evidenced by a reduction of HIV-induced cytopathogenic effects [43]]. Metabolite **17** was found to cause 23% inhibition of syncytia formation at concentrations of 3 µg/mL. Higher concentrations were not tested since it was found to be cytotoxic to the host cells at concentrations >6 µg/mL. Strong cytotoxicity at concentrations >0.8 µg/mL was also observed with enniatin B_1 (**19**) which was found to cause a 41% inhibition of the HIV protease enzyme at concentrations of 100 µg/mL.

CHAPTER 3

A Novel α-Pyrone from a Species of the *Trichoderma* Fungi

3.1 Introduction:

The genus *Trichoderma* is characterized by fast-growing fungi which are known to produce a large number of biologically active metabolites.[44] In the past, the *Trichoderma* fungi have often been explored as biological pest control agents.[45] For example, the potential use of *T. longibrachiatum* as a biofungicide (for the control of the American leaf spot disease caused by the fungus *Mycena citricolor* on coffee plants) was investigated and the antifungal agent trichodimerol (**31**) was isolated from its cultures.[46] Similarly, *T. harzianum*, a biological control agent of the plant pathogen *Pythium aphanidermatum*, has been studied and two antifungal metabolites, harzianopyridone (**32**) and harzianolide (**33**) were isolated.[47] In addition, several antibacterial agents have also been isolated from *Trichoderma* fungi including the isonitrile antibiotic trichoviridin (**34**), isolated from an unidentified *Trichoderma* species.[48]

In our studies, we have been investigating metabolites produced by a newly identified *Trichoderma* organism which exhibits strong cytotoxic activity against murine leukemic cells and human solid tumor cells. A biologically active mixture of metabolites was obtained from the liquid culture of this fungus which was purified by C18 reversed phase silica gel chromatography and LH-20 size exclusion column chromatography. The α-pyrone (**21**), a novel natural product, was isolated and characterized .

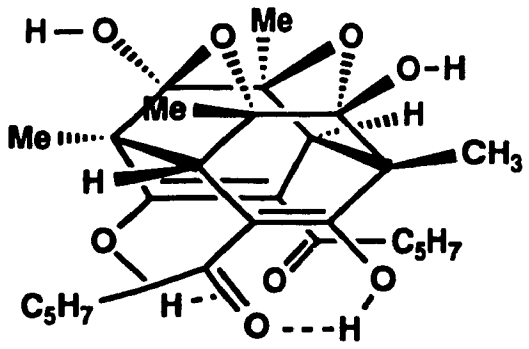

Trichodimerol (31)

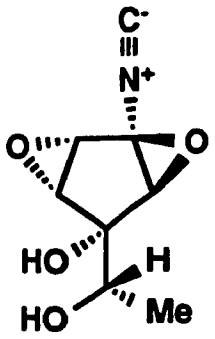

Trichoviridin (34)

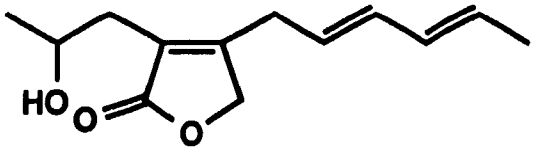

Harzianolide (32)

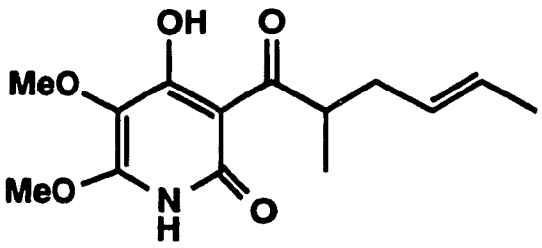

Harzianopyridone (33)

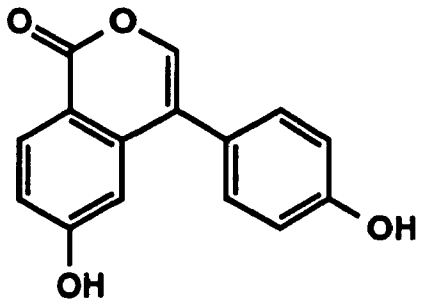

(21)

3.2 Results and Discussion:

Stock cultures of the *Tricoderma* fungus were maintained at 4°C in slant tubes containing 2% malt extract and 1.5% agar. A small amount of mycelium was used to inoculate plates (2% malt extract agar) which were then grown for 5 days at room temperature. Plugs of the actively growing mycelium were used to inoculate large scale liquid cultures which were incubated at 20°C on a rotary shaker for 7 days. At the end of the growth period, the mycelium was filtered through several layers of cheese cloth, the aqueous solution was reduced to about 20% of its original volume and freeze-dried to give a very fine, light-yellow, powder. MeOH was used to extract the crude metabolite mixture over a period of 24 hours. The methanolic solution (**Tc1**) was evaporated to dryness and the crude metabolite mixture was found to have strong cytotoxic activity (**Tab.6**) against both murine leukemic cells and human solid tumor cells. The metabolite mixture (**Tc1**) was further dissolved in deionized water (500 mL) and extracted with ethyl acetate (3 X 500 mL). The activity of the metabolites extracted into the ethyl acetate layer (**Tc2**) was found to be increased, whereas the water layer did not exhibit any activity (**Tab.6**).

The **Tc2** extract was purified by C18 reversed phased chromatography (20 mm x 20 cm) using a linear solvent gradient from 0.1% aqueous AcOH to 100% MeOH and then to 100% CH_2Cl_2. Two fractions were collected; **Tc2-1**, containing the metabolites which eluted from the column from the beginning up to a solvent mixture of H_2O:MeOH (1:1) and **Tc2-2** which contained the biologically active metabolites, along with all other components which eluted with a solvent mixture from H_2O:MeOH (1:1) to 100% CH_2Cl_2.

Table 6: Cytotoxic Activities of Tc1 and Tc2

Sample	IC_{50} (μg/mL)	Cell Lines
Tc1	3.29	P388D1 murine leukemic cells
	32	HEY human ovarian cells
	50	U373 human brain cells
	16.9	MCF human breast cells
	>50	A549 human lung cells
Tc2	0.025	P388D1 murine leukemic cells

Subsequently, the **Tc2-2** crude was dissolved in methanol and loaded on a Sephadex LH-20 column (25 mm x 45 cm) from which metabolite **21** was eluted with pure MeOH. Further purification was carried out after semi-preparative HPLC on a C18 reversed phase column. With a solvent mixture of 80% MeOH and 20% H_2O, the retention time for metabolite **21** was 7.02 min.

^1H NMR of metabolite **21** (**Tab.7**) revealed the presence of eight aromatic or olefinic protons between δ 6.88-8.13 (**Fig.26**); a doublet at δ 6.88 for two protons, a singlet at δ 6.89 and a doublet of doublets at δ 6.99 for one proton each, a doublet at δ 7.47 for two protons, a doublet at δ 8.05 for one proton and a singlet at δ 8.13 for a proton. The COSY NMR of metabolite **21** (**Fig.27**) clearly showed that the doublet at δ 8.05 (1H) was coupled to the doublet of doublets at δ 6.99 (1H) which was further coupled to a singlet (1H) at δ 6.89, suggesting an aromatic ring substituted at the two *para* positions and one of the *ortho* positions. The doublet at δ 7.47 (2H) was coupled to the

doublet (2H) at δ 6.88 suggesting an other *para*-substituted aromatic ring. However, the single proton at δ 8.13 was not coupled to anything else.

Thirteen non-equivalent carbons were observed in the ^{13}C NMR spectrum, (**Fig.28**). Six quaternary sp^2 carbons at δ 118.3, 124.5, 125.1, 158.0, 158.9, 163.7 of and an amide or ester carbon at δ 175.6. The chemical shift assignment of the protonated carbons was achieved by analysis of the HMQC NMR spectrum of metabolite **21** (**Fig.29**), whereas those of the quaternary signals were derived from the HMBC NMR data (**Fig.30**). For example, long range, ^3J coupling between the single proton at δ 8.13 and the ester (or amide) carbon, as well as the two quaternary carbons at δ 158.9 and 124.5, was observed. All of the NMR data of metabolite **21** are summarized in **Tab.7** and it is consistent with the α-pyrone stucture proposed (**21**). High resolution FAB MS of metabolite **21** gave a mass of 255.06575 for the $(M+H)^+$ molecular ion (calculated mass = 255.0657340) confirming an elemental composition of $C_{15}H_{10}O_4$.

Table 7: ^{1}H and ^{13}C NMR Data of Metabolite 21 (500MHz, CD_3COCD_3)

Carbon	$^{1}H(\delta)$	$^{13}C(\delta)$	COSY(δ)	HMBC(δ)
C-1		118.3		
C-2	8.05	128.4[a]	6.99	158.9, 163.7, 175.6
C-3	6.99	115.8[a]	6.89, 8.05	103.1, 118.3, 163.7
C-4		163.7		
C-5	6.89	103.1[a]	6.99	115.8, 118.3, 124.5, 158.9, 163.7
C-6		158.9		
C-7		175.6		
C-1'		124.5		
C-2'	7.47	131.0[a]	6.88	124.5, 125.1, 131.0
C-3'	6.88	115.7[a]	7.47	124.5, 158.0
C-4'		158.0		
C-5'	6.88	115.7[a]	7.47	124.5, 158.0
C-6'	7.47	131.0[a]	6.88	124.5, 125.1, 131.0
C-7'		125.1		
C-8'	8.13	153.0[a]		124.5, 158.9, 175.6

[a] Assignments based on the HMQC spectral data

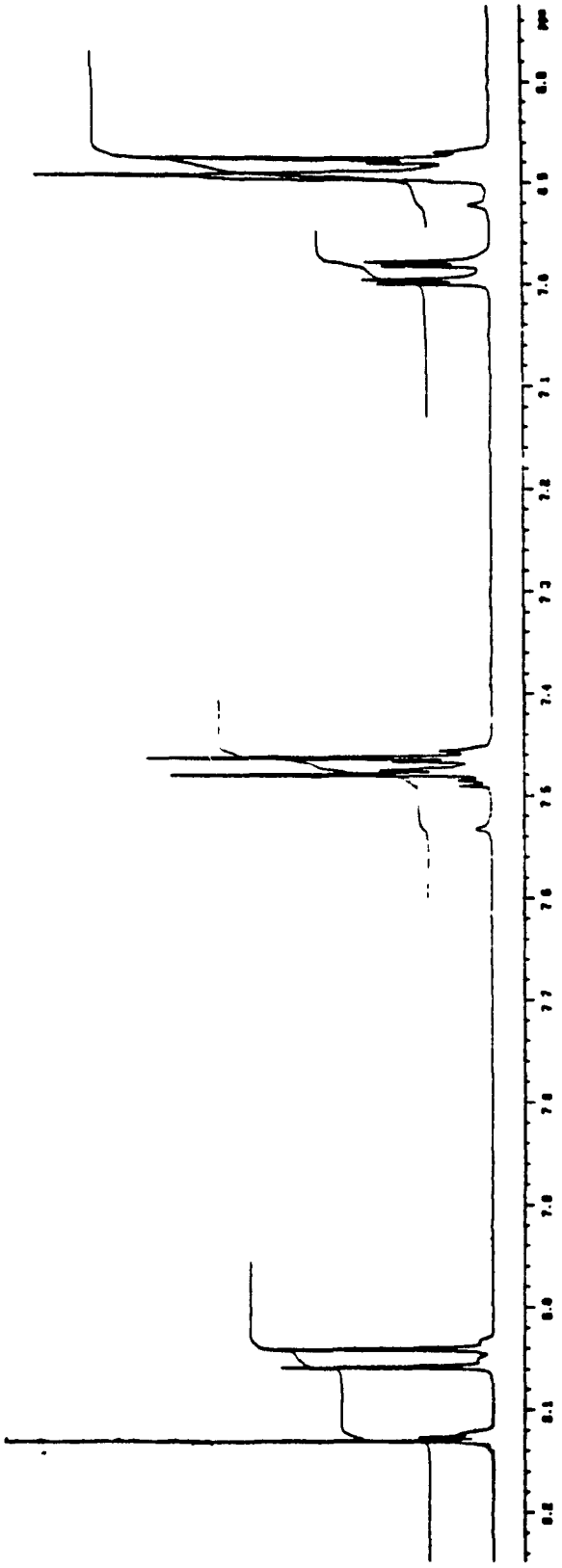

Figure 26: ^1H NMR (500 MHz, CD_3COCD_3) of Metabolite 21

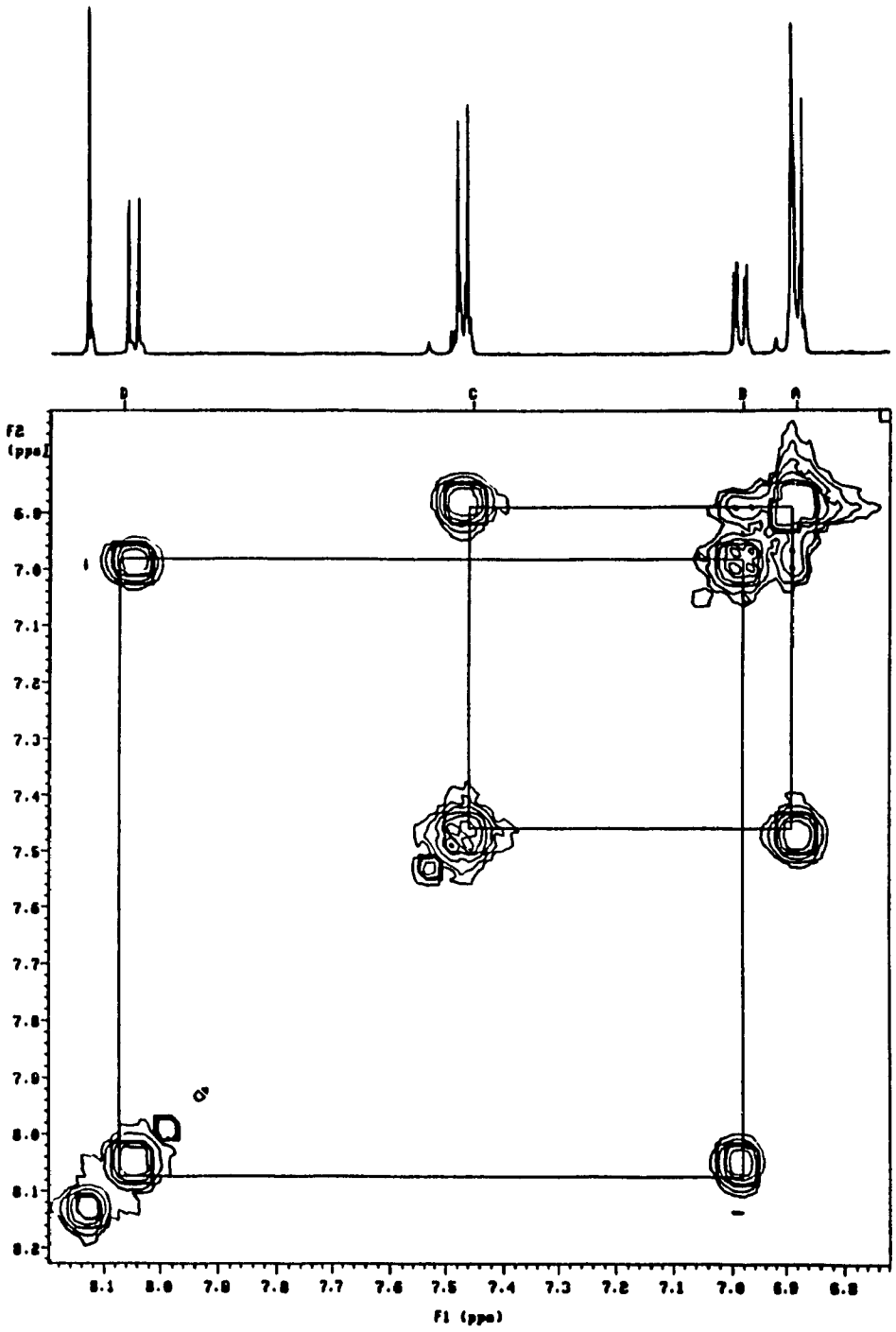

Figure 27: COSY NMR (500 MHz, CD_3COCD_3) of Metabolite 21

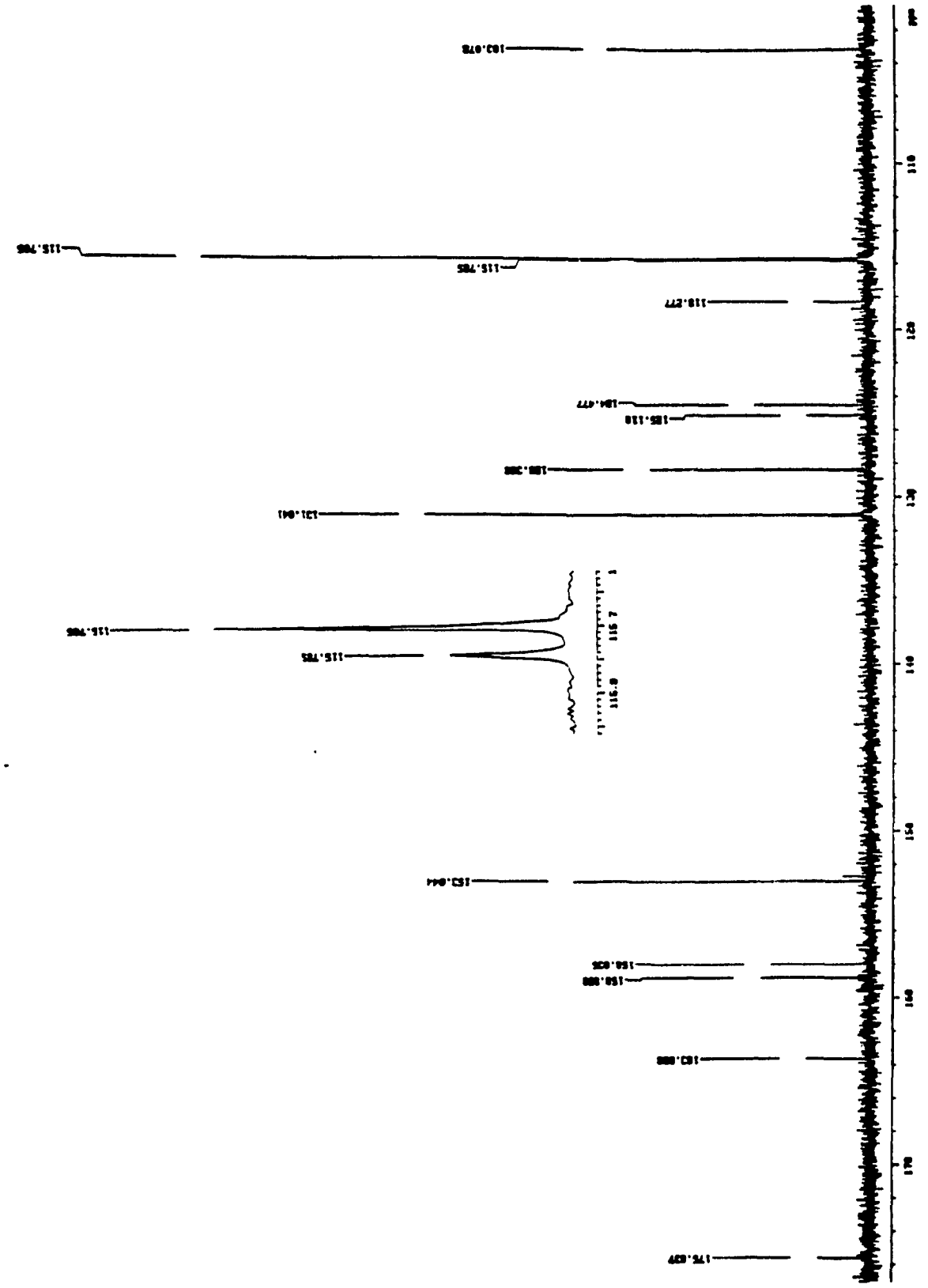

Figure 28: ^{13}C NMR (125 MHz, CD_3COCD_3) of Metabolite 21

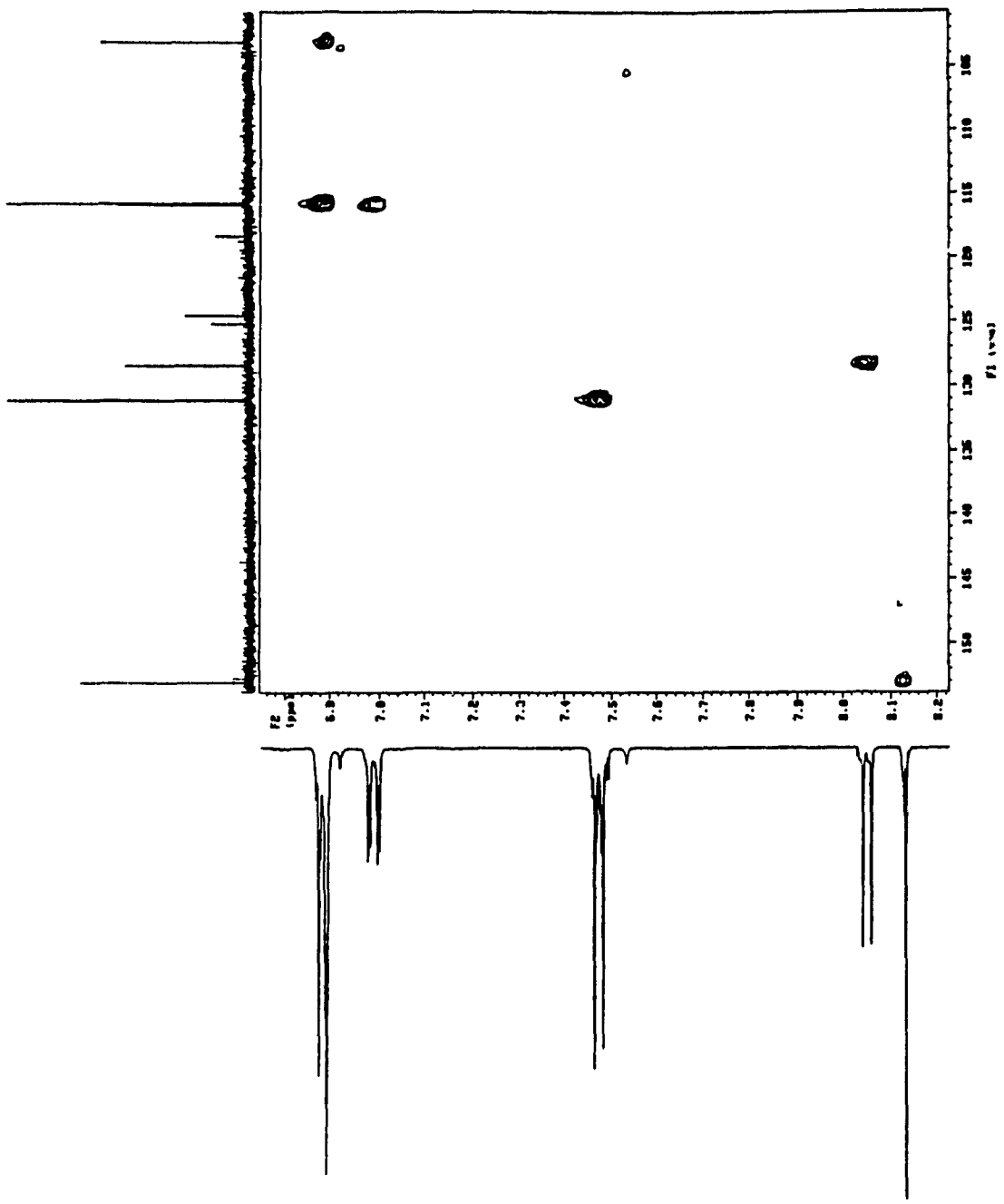

Figure 29: HMQC NMR (500 MHz, CD_3COCD_3) of Metabolite 21

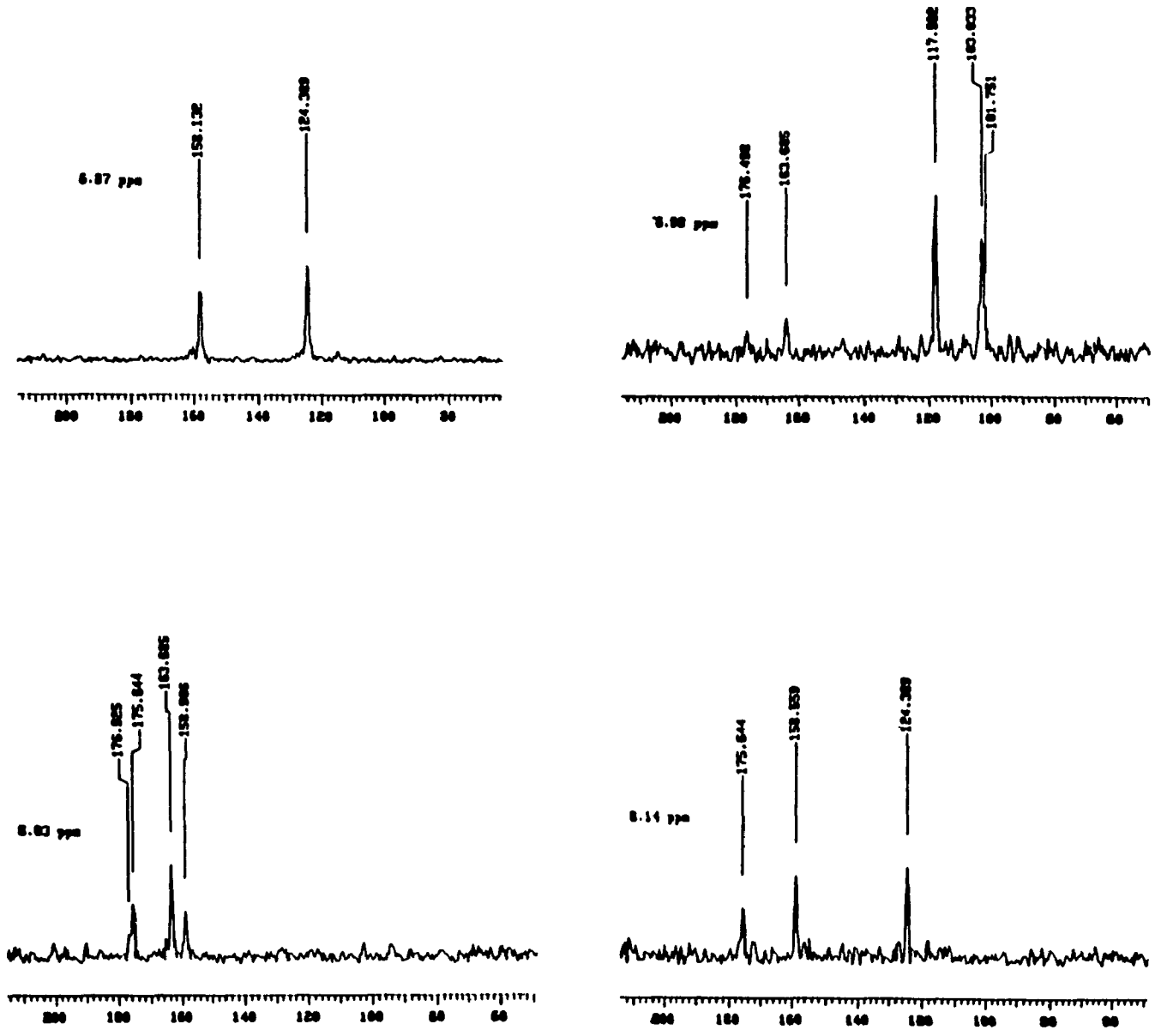

Figure 30: HMBC NMR (500 MHz, CD_3COCD_3) of Metabolite 21

CONTRIBUTIONS to KNOWLEDGE

The biologically active metabolites of *Fusarium lateritium* were investigated. Two novel alkaloids, 2(1-hydroxyethyl)-4(3H)quinazolinone and 2-acetyl-4(3H)-quinazolinone, were isolated and characterized. In addition, the production of enniatins B, B_1 and A_1 by *F. lateritium* were shown to be responsible for the antagonistic effects of this organism against the serious plant pathogen *Eutypa armeniacae.*

The biologically active metabolites of a second organism, a fungus from the *Trichoderma* species, were also investigated. A crude metabolite mixture from this organism was shown to exhibit potent antitumor activity and a novel α-pyrone metabolite was isolated from this mixture and characterized.

CHAPTER 4

EXPERIMENTAL

4.1 General Methods:

Spectra:

Nuclear Magnetic Resonance spectra were obtained at 20-22°C using JEOL 270 MHz-CPF, Varian XL-200 MHz, Varian XL-300 MHz and Varian Unity 500 MHz instruments. ^{1}H and ^{13}C-NMR chemical shifts are quoted in ppm and are referenced to the internal deuterated solvent downfield from tetramethylsilane (TMS). ^{19}F NMR was recorded in $CDCl_3$; $CFCl_3$ was used as an external reference.

Mass spectra were performed at the Biomedical Mass Spectrometry Unit, McGill University and the Mass Spectrometry Centre, Department of Chemistry, University of Ottawa. FAB MS [Cs^+ particles, diethanolamine matrix] spectra were obtained using a Concept 2H Kratos instrument, EI MS spectra were obtained using a VG 7070 instrument and high resolution $(NH_3)CI$ MS spectra were obtained using a ZAB 2F HS instrument (resolution: 10^4).

Melting points were measured using a Gallenkamp capillary apparatus and they are uncorrected. Ultraviolet spectra were recorded on a Hewlett Packard 8452A DIODE ARRAY Spectrophotometer. Infrared spectra were recorded on a Bomem Michelson 102 FTIR spectrophotometer calibrated to the 1602 cm^{-1} line of polystyrene.

Chromatography:

Reverse phase flash column chromatography was carried out on silica gel (Merck Kieselgel 60, 230-400 mesh, #9385) reacted with *n*-octadecyltrichlorosilane. C18 reverse-phase silica gel was prepared following previously reported procedures.[27] Thin layer chromatography (TLC) was performed on Merck RP-18F_{254s} plates (0.25 mm thickness). Gel filtration column chromatography was carried on using Sephadex LH-20 purchased from Pharmacia LKB Biotechnology Inc.

HPLC:

NANOpure H_2O and HPLC grade MeOH and MeCN, were filtered through a 0.45 μ filter membrane (Millipore Corp., Bedford, MA) before they were used in HPLC. Analysis and purification was carried out on a semi-preparative reverse phase, C18 column; Waters NOVA-PAK (25 mm x 100 mm, 6μm, 60Å) using a Waters instrument (pump model W600EP, UV/VIS detector model M486P, Rheodyne injector). All retention times were automatically recorded from the time of injection.

Preparation of C18 Reversed Phase Silica Gel:[27]

Silica gel (80 grams, Merck Kieselgel 60, 230-400 mesh) was added to 400 mL dry CCl_4 (distilled from P_2O_5) in a septum-capped round bottom flask. *n*-Octadecyltrichlorosilane (8 mL) was added and the suspension was stirred at room temperature for two hours.

The product was filtered into a dry seinterglass funnel and washed free of unreacted silane with dry CCl_4 (3 x 100 mL). Any residual chloride substitutes were converted to methoxy group by washing the silica with dry methanol (2 x

200 mL, distilled over Mg metal). The product was then quickly washed with dry CH_2Cl_2 (2 x 200 mL, redistilled from P_2O_5) and allowed to briefly dry under vacuum.

A fresh 400 mL volume of dry CCl_4 was added to the bonded silica along with 8 mL of trimethylchlorosilane. The mixture was stirred at room temperature for an additional two hours, then filtered and washed with dry CH_2Cl_2 (3 x 150 mL). The bonded silica was briefly dried under high vacuum for 24 hours.

HMQC, HMBC:

HMQC whose abbreviation is heteronuclear multiple-quantum coherence was first proposed by Muller. The experiment can identify $^1J_{CH}$ coupling by detection through ^1H nuclei. This method provides sensitivity enhancement in a short period of time with small amounts of samples, however it can't allow the assignment of non-protonated carbons. Heteronuclear multiple bond connectivity (HMBC), which is a modification of the HMQC experiment , can detect $^2J_{CH}$ and $^3J_{CH}$ coupling. It has the same advantages as HMQC; a small amount of products can be detected sensitively in a short period of time. For example, compound **16** , in HMBC experiment , H-2' is coupled to both C-1' and C-2; H-1' is coupled to C-2' and C-2.

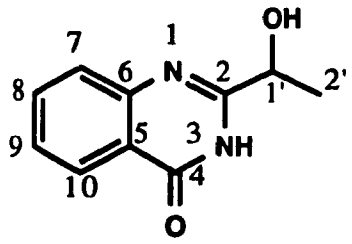

4.2 Novel Quinazolinones and Enniatins from *F. lateritium* :

Stock cultures of *F. lateritium* were maintained on Czapex-Dox (Difco) plus 5% yeast agar in slant tubes at 4°C. A small amount of mycelium was used to inoculate 45 Czapex-Dox plus 5% yeast agar plates which were then incubated in the dark, at room temperature for a period of 5 weeks. A crude metabolite mixture was isolated from the infected agar plates by soaking the agar in CH_2Cl_2 (2x500 mL) over a period of 24 h. Evaporation of the CH_2Cl_2 led to the isolation of a metabolite mixture (~240 mg) exhibiting strong antifungal activity against *E. armeniacae*.

The crude metabolite mixture was first purified by flash column chromatography on a C18 reversed phase column (20 mm x 20 cm),[27] using a linear solvent gradient from 0.1% aqueous AcOH to 100% MeOH, at a flow rate of ~4 cm/min. Metabolites **16** and **17** eluted from the column in 45-55% and 60-70% aqueous MeOH respectively, while metabolites **18** and **19** and **20** eluted in 80-100% aqueous MeOH. Metabolite **16** was further purified by normal phase flash column chromatography using EtOAc , whereas metabolite **17** was purified by crystallization from CH_2Cl_2. Approximately 5-8 mg of each metabolite **16** and **17** were isolated from 40 plates of *F. lateritium*. Pure metabolites **18**, **19** and **20** were isolated after semi-preparative HPLC on a C18 reverse phase column, eluted with 55% MeOH, 15% H_2O and 30% MeCN. At a flow rate of 5 mL/min, the retention times for metabolites **18**, **19** and **20** were 22-23 min, 26-27 and 33-34 min respectively. The yields of pure enniatins isolated from 40 infected plates were approximatly 12 mg of B (**18**), 15 mg of B_1 (**19**) and 3 mg of A_1 (**20**).

2(1-hydroxyethyl)-4(3H)quinazolinone (16)

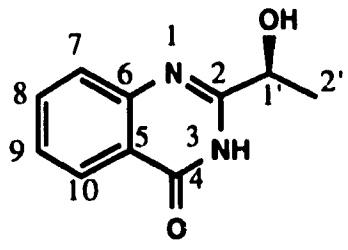

TLC: EtOAc, Rf=0.34.

M.p.: 155-156°C

UV (MeOH, nm): max 226, min 264, 304.

IR (MeCN): 3550, 3542 (OH, NH), 1690 (-CO-NH-), and 1605 (C=N) cm^{-1}.

$[\alpha]_D$ -26.6 (the calculated $[\alpha]_D$ for the R enantiomer was based on ~20% ee of R in the sample of metabolite **16** isolated, *c* 0.258, MeOH, 20°C).

^{1}H NMR (500 MHz, CD_3OD) δ: 1.53 (d, J=6.6 Hz, 3H, -C<u>H</u>$_3$), 4.73 (q, J=6.6 Hz, 1H, C<u>H</u>-OH), 7.49 (ddd, J_{9-10}=8.1 Hz, J_{8-9}=7.8 Hz, J_{7-9}=2.4 Hz, 1H, H-9), 7.66 (d, J_{7-8}=8.1 Hz, 1H, H-7), 7.79 (ddd, J_{7-8}=8.1 Hz, J_{8-9}=7.8 Hz J_{8-10}=2.3 Hz, 1H, H-8) and 8.18 (dd, J_{9-10}=8.1 Hz, J_{8-10}=2.3 Hz, 1H, H-10) ppm.

^{13}C NMR (125 MHz, CD_3OD) δ: 22.4 (C-2'), 68.6 (C-1'), 122.2 (C-5), 127.2 (C-10), 127.5 (C-7), 127.8 (C-9), 135.9 (C-8), 149.6 (C-6), 161.6 (C-2) and 164.3 (C-4) ppm.

MS [HR, (NH_3)Cl]: m/z calculated for (M^++1) ion 191.08205, found 191.08201.

Preparation of the (S)-MTPA-ester-16

(R)-MTPA chloride (10 µL, 52 µmol) was added to a solution of **16** (3.3 mg, 17.4 µmol) in pyridine (~100 µL). After the reaction mixture was allowed to stir at room temperature for 15 h, it was diluted with 10 mL CH_2Cl_2 and the pyridine was removed by extraction with 5% aqueous $CuSO_4$ solution (3 x 10 mL). The

residue obtained from the CH_2Cl_2 layer after evaporation was purified by preparative TLC [CH_2Cl_2-EtOAc (1:1), Rf = 0.75].

^{1}H NMR (270 MHz, $CDCl_3$): δ 1.63 and 1.71 (d, J=6.6 Hz, ratio=~1:1.5, Me), 3.49 and 3.55 (s, ratio=~1:1.5, -OMe), 5.9 (m, carbinol C<u>H</u>), 7.3-8.2 (overlapping aromatic signals), 8.9 and 9.2 (s, ratio=~1.5:1, -CON<u>H</u>-) ppm.

^{19}F NMR (300 MHz, $CDCl_3$): δ -71.7 and -71.4 (ratio=1.5:1) ppm.

2-Acetyl-4(3H)quinazolinone (17)

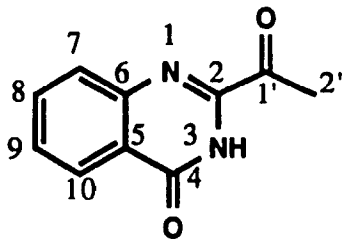

TLC: CH_2Cl_2 / EtOAc (3:1), Rf=0.59.

M.p.: 188.0-188.5°C

IR ($CDCl_3$): 3351 (NH), 1692 (-CO-NH- and -CO-Me) and 1606 (C=N) cm^{-1}.

UV (H_2O, nm): max 232, min 302.

^{1}H NMR (200 MHz, $CDCl_3$): δ 2.75 (s, 3H, -CO-C<u>H</u>$_3$), 7.60 (ddd, $J_{9\text{-}10}$=8.0 Hz, $J_{8\text{-}9}$=6.1 Hz, $J_{7\text{-}9}$=2.3 Hz, 1H, H-9), 7.78-7.88 (m, 2H, H-7&H-8), 8.33 (dd, $J_{9\text{-}10}$=8.0 Hz, $J_{8\text{-}10}$=2.3 Hz, 1H, H-10) and ~9.9 (bs, 1H, CO-N<u>H</u>) ppm.

^{13}C NMR (67.5 MHz, CDCl3) δ: 24.5 (C-2'), 123.5 (C-5), 126.9 (C-10), 129.2 (C-7), 129.4 (C-10), 134.8 (C-8), 145.3 (C-6), 147.7 (C-2), 160.5 (C-4) and 194.1 (C-1') ppm.

MS [EI, VG 7070E Mass Spectrometer], m/z (% relative intensity, assignment): 189 (100, M^++1), 175 [25, (M^++1)-CH_2], 133 [20, (M^++1)-(CH-CO-CH_3)].

Enniatin B (18)

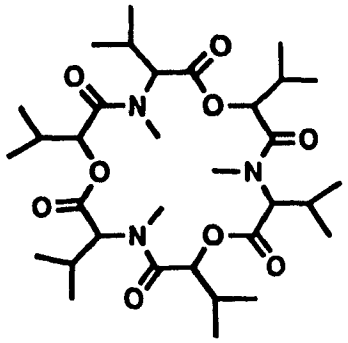

TLC: CH_2Cl_2 / EtOAc (1:3), Rf=~0.73.

M.p.: 167-169°C

IR ($CHCl_3$): 1664 (C=O, amide) and 1732 (C=O, ester) cm^{-1}.

$[\alpha]_D$ -114.6 (*c* 0.32, $CHCl_3$, 20°C).

^{1}H NMR (500 MHz, $CDCl_3$):

N-Me-Val δ: 0.88 (d, $J_{\beta-\gamma}$=6.8 Hz, 3H, γ-Me), 1.05 (d, $J_{\beta-\gamma}$=6.3 Hz, 3H, γ-Me), 2.29 (m, 1H,* β-H), 3.12 (s, 3H, N-Me), 4.51 (d, $J_{\alpha-\beta}$=9.3 Hz, 1H, α-H) ppm.

Hiv δ: 0.95 (d, $H_{\beta-\gamma}$=6.8 Hz, 3H, γ-Me), 0.97 (d, $J_{\beta-\gamma}$=5.9 Hz, 3H, γ-Me), 2.26 (m,1H,* β-H), 5.13 (d, $J_{\alpha-\beta}$=8.8 Hz, 1H, α-H) ppm.

^{13}C NMR& (125 MHz, $CDCl_3$):

N-Me-Val δ: 19.1 and 20.2 (2 γ-Me), 27.7 (β-C), 33.1 (N-Me), 63.0 (α-C) and 169.1 (C=O, amide) ppm.

Hiv δ: 18.3 and 18.5 (2 γ-Me), 29.7 (β-C), 75.5 (α-C) and 170.1 (C=O, ester) ppm.

FAB MS [Cs^+ particles, diethanolamine matrix], m/z (assignment): 640 $(M+H)^+$, 662 $(M+Na)^+$, 678 $(M+K)^+$, 745$(M+DEA+H)^+$, 772 $(M+Cs)^+$.

Enniatin B_1 (19)

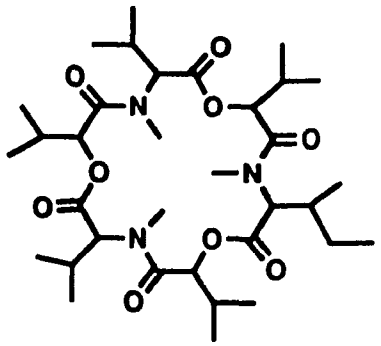

TLC: CH_2Cl_2 / EtOAc (1:3), Rf=~0.73.

M.p.: 122-123°C

IR ($CHCl_3$): 1664 (C=O, amide) and 1732 (C=O, ester) cm^{-1}.

$[\alpha]_D$ -106.7 (*c* 0.34, $CHCl_3$, 20°C).#

^{1}H NMR (500 MHz, $CDCl_3$):

N-Me-Val δ: 0.88 (d, $J_{\beta-\gamma}$=6.8 Hz, 3H, γ-Me), 1.05 (d,$J_{\beta-\gamma}$=6.4 Hz, 3H, γ-Me), 2.30 (m, 2H,* β-H), 3.12 [s, 6H, 2(N-Me)], 4.45 (d, $J_{\alpha-\beta}$=9.3 Hz, 1H, α-H), 4.50 (d, $J_{\alpha-\beta}$=9.8 Hz, 1H, α-H) ppm.

Hiv δ: 0.93-0.99 (6d, $J_{\beta-\gamma}$=6-8 Hz,* 18H, 6γ-Me), 2.27 (m, 3H,* 3β-H), 5.09 (d, $J_{\alpha-\beta}$=9.3 Hz, 1H, α-H), 5.12 (d, $J_{\alpha-\beta}$=8.8 Hz, 1H, α-H), 5.15 (d, $J_{\alpha-\beta}$=8.8 Hz, 1H, α-H) ppm.

N-Me-ILe δ: 0.86 (t, $J_{\gamma-\delta}$=7.6 Hz, 3H, δ-Me), 0.99 (d, $J_{\beta-\gamma}$=6.8 Hz, 3H, γ-Me), 1.10 & 1.41 (2m, γ-CH_2), 2.07 (m, 1H, β-H), 3.10 (s, 3H, N-Me), 4.72 (d, $J_{\alpha-\beta}$=9.3 Hz, α-H).

^{13}C NMR[&] (125 MHz, $CDCl_3$):

N-Me-Val δ: 19.2 and 20.3 (4 γ-Me), 27.8 and 27.9 (2 β-C), 33.2 and 33.3 (2 N-Me), 63.1 and 63.3 (2 α-C) and 169.0 (2 C=O, amide) ppm.

Hiv δ: 18.2, 18.3 and 18.5 (6 γ-Me), 29.7 (3 β-C), 75.2 and 75.6 (3 α-C) and 170.1 and 170.2 (3 C=O, ester) ppm.

N-Me-ILe δ: 10.7 (δ-Me), 16.0 (γ-Me), 25.1 (γ-CH_2), 32.5 (N-Me), 33.7 (β-C), 61.2 (α-C), 169.0 (C=O, amide) ppm.

FAB MS [Cs^+ particles, diethanolamine matrix], m/z (assignment): 654 $(M+H)^+$, 676 $(M+Na)^+$, 692 $(M+K)^+$, 759 $(M+DEA+H)^+$, 786 $(M+Cs)^+$.

Enniatin A_1 (20)

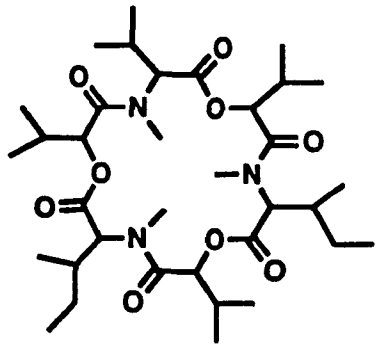

TLC: CH_2Cl_2 / EtOAc (1:3), Rf=~0.73.

IR ($CHCl_3$): 1664 (C=O, amide) and 1732 (C=O, ester) cm^{-1}.

$[\alpha]_D$ -110.9 (*c* 0.08, $CHCl_3$, 20°C).

^{1}H NMR (500 MHz, $CDCl_3$):

N-Me-Val δ: 0.90 (d, $J_{\beta-\gamma}$=7.3 Hz, 3H, γ-Me), 1.07 (d,

$J_{\beta-\gamma}$=6.3 Hz, 3H, γ-Me), 2.31 (m, 1H,* β-H), 3.14 (s, 3H, N-Me), 4.45 (d, $J_{\alpha-\beta}$=9.3 Hz, 1H, α-H) ppm.

Hiv δ: 0.94-1.00 (6d, $J_{\beta-\gamma}$=6-8 Hz,* 18H, 6 γ-Me), 2.26 (m, 3H,* 3 β-H), 5.09 (d, $J_{\alpha-\beta}$=8.3 Hz, 1H, α-H), 5.12 (d, $J_{\alpha-\beta}$=8.3 Hz, 1H, α-H), 5.15 (d, $J_{\alpha-\beta}$=8.9 Hz, 1H, α-H) ppm.

N-Me-ILe δ: 0.86 (t, $J_{\gamma-\delta}$=7.3 Hz, 6H, 2 δ-Me), 1.00 (d, $J_{\beta-\gamma}$=6.3 Hz, 6H, γ-Me), 1.08 & 1.41 (2m, 4H, 2 γ-CH_2), 2.06 (m, 2H, 2β-H), 3.11 (s, 6H, 2 N-Me), 4.69 (d, $J_{\alpha-\beta}$=12.0 Hz, 1H, α-H), 4.71 (d, $J_{\alpha-\beta}$=11.2 Hz, 1H, α-H) ppm.

^{13}C NMR[&] (125 MHz, $CDCl_3$):

N-Me-Val δ: 19.3 and 20.4 (2 γ-Me), 27.9 (β-C), 33.4 (N-Me), 63.4 (α-C) and 169.1 (2 C=O, amide) ppm.

Hiv δ: 18.3, 18.4 and 18.5 (6 γ-Me), 29.7 (3 β-C), 75.3 and 75.8 (3 α-C) and 170.1 and 170.2 (3 C=O, ester) ppm.

N-Me-ILe δ: 10.7 (2 δ-Me), 16.0 (2 γ-Me), 25.2 (2 γ-CH_2), 32.6 (2 N-Me), 33.7 and 33.8 (2 β-C), 61.4 and 61.5 (2 α-C), 169.1 (2 C=O, amide) ppm.

FAB MS [Cs^+ particles, diethanolamine matrix], m/z (assignment): 668 $(M+H)^+$, 690 $(M+Na)^+$, 706 $(M+K)^+$, 773 $(M+DEA+H)^+$, 800 $(M+Cs)^+$; [Cs^+ particles, glycerol matrix], m/z (assignment): 668 $(M+H)^+$.

---

* Overlapping signals; integration and/or J values not clear.[#] Enniatin B_1 was isolated by Blackwell, Miller and coworkers[22] as a pale yellow oil having $[\alpha]_D$ +173.8, however, the sign of the optical rotation is a typographical error (private communication). [&] Assignments based on the HMQC and HMBC NMR data.

Bioassays against *E. armeniacae*

Biological testing of enniatins B (**18**), B_1 (**19**) and A_1 (**20**) for their ability to inhibit the grown of *E. armeniacae* were carried out on Czapex-Dox plus 5% yeast agar plates. Samples of each compound ranging in amounts from 8 - 170 μg were absorbed onto sterile paper disks and each was placed at the edge of a sterile plate. The plates were inoculated at the center with a constant size plug of *E. armeniacae* mycelium, cut from the edge of an actively grown colony of this fungus. The inhibition zone from the center of the paper disk to the edge of the *E. armeniacae* growth was measured from 1 to 3 days after the growth on the control plates had reached its maximum (*i.e.*, plates were completely covered with mycelium) (**Fig.31**).

Initially, all samples showed an inhibition zone of 8-14 mm, however, after an incubation period of ~15 days there was little or no inhibition observed with enniatins B and B_1, whereas the plates tested with enniatin A_1 showed a consistent and persisting inhibition zone of 5-10 mm. The difference observed between the 8 μg and the 170 μg samples was very small, most likely due to the poor solubility and absorption of the compounds into the agar medium, thus a dose *versus* inhibition response could not be evaluated.

Figure 31: Antifungal Bioassay of Enniatins against *E. armeniacae*

(left: control; right: 8 μg of enniatin A_1)

4.3 A Novel α-Pyrone from a Species of the *Trichoderma* Fungi

4.3.1 Growth and Isolation of a Crude Metabolite Mixture from a new Species of the *Trichoderma* Fungi

Stock cultures of the *Tricoderma* fungus were maintained at 4°C in slant tubes containing 2% malt extract and 1.5% agar. A small amount of mycelium was used to inoculate agar plates (2% malt extract) which were then grown for 5 days. Plugs (15/flask) of the actively grown mycelium were used to inoculate large scale liquid medium (6x500 mL 2% malt extract). These were then incubated at 20°C on a rotary shaker at 120 rpm for 7 days. Mycelium was filtered through several layers of cheese cloth and the aqueous solution was reduced in volume (~1/5) at 35°C under high vacuum. The remaining water was lyophilized to give a solid. The powder was extracted with MeOH (2x1000 mL) over a period of 24 hours. The methanolic solution was filtered through filter paper to remove the undissolved solid material. The methanol was evaporated to dryness to give 44 g of a crude metabolite mixture (**Tc1**). The mixture of metabolites was dissolved in 500 mL deionized water and then extracted with EtOAc (3x500 mL) over a period of 24 hours. The organic layer was subsequently dried with $MgSO_4$ and evaporated to give ~210 mg of an oily crude (**Tc2**). The water layer was found to be void of any significant biological activity, therefore it was not analyzed any further.

4.3.2 C18 Reversed Phase Column on Tc1

A C18 reversed phase column (27 mm x 20 cm, ~53 grams C18 silica) was packed and equilibrated as the same way described before. The **Tc1**

metabolite mixture (11 g) was applied on the column and 12 fractions were collected and the IC_{50} values as shown in **Tab.8**:

Table 8: C18 Reversed Phase Column on Tc1 and IC_{50} Values

Fraction	Solvent System	IC_{50} (μg/mL)
Fraction-1	100 mL H_2O*	>50
Fraction-2	100 mL H_2O	>50
Fraction-3	100 mL H_2O:MeOH=3:1	>50
Fraction-4	100 mL H_2O:MeOH=3:2	>50
Fraction-5	100 mL H_2O:MeOH=2:3	>50
Fraction-6	100 mL H_2O:MeOH=1:4	>50
Fraction-7	100 mL H_2O:MeOH=1:9	>50
Fraction-8	100 mL MeOH	0.69
Fraction-9	100 mL MeOH:CH_2Cl_2=9:1	0.009
Fraction-10	100 mL MeOH:CH_2Cl_2=3:1	0.01
Fraction-11	100 mL MeOH:CH_2Cl_2=1:1	0.096
Fraction-12	200 mL CH_2Cl_2	0.53

* H_2O with 0.1% aqueous CH_3COOH.

4.3.3 Isolation of Metabolite 21

4.3.3a C18 Reversed Phase Column on Tc2

A reversed phase column (20 mm x20 cm) was packed and equilibrated as the same way described before. 210 mg **Tc2** was applied on the column and eluted with a linear solvent gradient from 0.1% aqueous AcOH to 100% MeOH and to 100% CH_2Cl_2. Two fractions were collected: the first one (**Tc2-1**) was collected from the beginning of the column to H_2O: MeOH (1:1); and the second fraction (**Tc2-2**) was from H_2O: MeOH (1:1) to the end (100% CH_2Cl_2). The latter fraction contained the biologically active metabolites.

4.3.3b Purification of Metabolite 21

The active metabolite mixture **Tc2-2** (~37 mg) was dissolved in 5 mL MeOH and loaded on a Sephadex LH-20 column (20 mm x 45 cm). The column was eluted with pure MeOH and 90 fractions (~2.5 mL each) were collected. Metabolite **21** (~3.1 mg) eluted from the column in fractions 79-84. Further purification was carried out after semi-preparative HPLC on a C18 reversed phase column. A solvent mixture of 80% MeOH and 20% H_2O was used. The UV detector was set at 250 nm. At a flow rate of 5 mL/min, the retention time for metabolite **21** was 7.02 min.

Metabolite (21)

TLC: EtOAc, Rf=0.56.

UV (MeOH, nm): max 250, min 208, 304.

^{1}H NMR (500 MHz, CD_3COCD_3) δ: 6.88 (d, J=8.79 Hz, 2H, H-3' & H-5'), 6.89 (s, 1H,

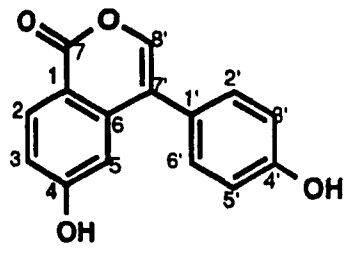

H-5), 6.99 (dd, J_{2-3}=8.79 Hz, J_{3-5}=2.20 Hz, 1H, H-3), 7.47 (d, J=8.79 Hz, 2H, H-2' & H-6'), 8.05 (d, J=8.79 Hz, 1H, H-2) and 8.13 (s, 1H, H-8') ppm.

^{13}C NMR (125 MHz, CD_3COCD_3) δ: 103.1 (C-5), 115.7 (C-3' &C-5'), 115.8 (C-3), 118.3 (C-1), 124.5 (C-1'), 125.1 (C-7'), 128.4 (C-2), 131.1 (C-2' &C-6'), 153.0 (C-8'), 158.0 (C-4'), 158.9 (C-6), 163.7 (C-4) and 175.6 (C-7) ppm.

MS [high resolution, $(NH_3)Cl$]: m/z calculated for (M^++1) ion 255.06573, found 255.06575.

4.3.4 Bioassay of Tc1 and Tc2

The bioassays on leukemic cells and human solid tumor cells were performed by Dr. Theresa Allen, Department of Pharmacology, University of Alberta and Dr. Brian Leyland-Jones, Department of Oncology, McGill University.

The IC_{50} values obtained from bioassays using P388D1 or L1210 murine leukemic cell for the crude metabolite mixtures of **Tc1** and **Tc2** were 3.62 μg/mL and 0.025 μg/mL respectively. The IC_{50} value obtained after C18 reversed phase column chromatography of crude **Tc1** are shown in **Tab.8**.

The crude metabolite mixture **Tc1** was found to be also cytotoxic to a number of important human carcinoma cell lines; HEY human ovarian cells (IC_{50}=32 μg/mL), U373 human brain cells (IC_{50}=50 μg/mL) and MCF human breast cells (IC_{50}=16.9 μg/mL).

REFERENCES:

1. J. Mann, *Secondary Metabolite* (2nd edition) pp 1-22, Oxford University Press.

2. K.K. Chen, *J. Am. Pharm. Assoc.* **14**, 189 (1925).

3. Y.S.Tantrizos, *Natural Products*, pp39.

4. M.D.Lee, J.K.Manning, D.R.William, W.A.Kuck, R.T.Testa and D.B.Borders, *J. Antibiotics* **XLII**, 1070-1087 (1989).

5. A.Stierle, G.Strobel and D.Stierle, *Science*, **260**, 214 (1993).

6. M.Konishi, H.Ohkuma, K.Saitoh, H.Kawaguchi, J.Golik, G.Dubay, G.Groenewold, B.Krishnan and T.W.Doyle. *J. Antibiot.* **38**, 1605 (1985).

7. M.Konishi, H.Ohkuma, K.Matsumoto, T.Tsuno, H.Kamei, T.Miyaki, T.Oki, H.Kawaguchi, G.D.Van Duyne and J.Clardy. *J.Antibiot.* **42**, 1449 (1989).

8. K.C.Nicolaou, G.Zuccarello, C.Riemer, V.A.Estevez and W.-M.Dai, *J. Am. Chem. Soc.* **114**, 7360 (1992).

9. R.B.Silverman, *The Organic Chemistry of Drug Design and Drug Action*, pp 235-276, Academic Press.

10. B.H.Long, J.Golik, S.Forenza, B.Ward, R.Rehfuss, J.C. Dabrowiak, J.J.Catino, S.T.Musial, K.W.Brookshire and T.W.Doyle, *Proc. Natl. Acad. Sci. U.S.A.* **86**, 2 (1987).

11. N.Zein, A.M.Sinha, W.J.McGahren and G.A.Ellestad, *Science*, **240**, 1198 (1988).

12. R.R.Jones, R.G.Bergman, *J. Am. Chem. Soc.* **94**, 660 (1972).

13. H.T.Dulmage, *Microbial control of pests and plant diseases* 1970-1980 (H.D.Burges, ed.) pp 193-222, Academic Press, London.

14. A.S.Moffat, *Science*, **252**, 211 (1991).

15. M.Reisch, *C&EN*, Oct.29, 6 (1990).

16. S.Gopalakrishnan, M.P.Stone and T.M.Harris, *J. Am. Chem. Soc.* **111**, 7232 (1989).

17. a) M.V. Carter. *Aust. J. Exp. Agric. Anim. Husb.* **23**, 429 (1983).
b) M.V. Carter and T.V. Price. *Aust. J. Agric. Res.* **26**, 537 (1975).

18. E.H. Gendloff, D.C. Ramsdell and C.L. Burton. *Plant Disease* **67**, 754 (1983).

19. E. Gaumann, S. Roth, L. Ettlinger, P.A. Plattner and U. Nager. *Experientia* **3**, 202 (1947).

20. A. Visconti, L.A. Blais, J.W. ApSimon, R. Greenhalgh and J.D. Miller. *J. Agric. Food Chem.* **40**, 1076 (1992).

21. Y.S. Tsantrizos, X.-J. Xu, F. Sauriol and R.C. Hynes. *Can. J. Chem.* **71**, 1362 (1993).

22. L.A. Blais, J.W. ApSimon, B.A. Blackwell, R. Greenhalgh and J.D. Miller. *Can. J. Chem.* **70**, 1281 (1992).

23. (a) H.L. Walker, *Weed Sci.* **29**, 629 (1981).
(b) Eur. Pat. 207653 A 17 Jan. 1987
(c) US Pat. 85-747511 21 Jun. 1985

24. (a) C.P. Gorst-Allman, P.H. van Rooyen, S. Wnuk, P. Golinski and J. Chelkowski. *S.-Afr. Tydskr. Chem.* **39**, 116 (1986).
(b) G.W. Bushnell, Y.-L. Li and G.A. Poulton. *Can. J. Chem.* **62**, 2101 (1984).

25. M. Cole and G.N. Rolinson. *Appl. Microbiol.* **24**, 660 (1972).

26. G.C. Bishop and A.H. Isley. *Aust. J. Biol. Sci.* **31**, 93 (1978).

27. (a) Y.S. Tsantrizos, K.K. Ogilvie and A.K. Watson. *Can. J. Chem.* **70**, 2276 (1992).
(b) J.W. Blunt, V.L. Calder, G.D. Fenwick, R.J. Lake, J.D. McCombs, M.H.G. Munro and N.B. Perry. *J. Nat. Prod.* **50**, 290 (1987).

28. (a) J.A. Dale and H.S. Mosher. J. Am. Chem. Soc. 95, 512 (1973). (b) G.R. Sullivan, J.A. Dale and H.S. Mosher. *J. Org. Chem.* **38**, 2143 (1973).

29. I. Ohtani, T. Kusumi, Y. Kashman and H. Kakisawa. *J. Am. Chem. Soc.* **113**, 4092 (1991).

30. M.J. Rieser, Y. Hui, J.K. Rupprecht, J.F. Kozlowski, K.V. Wood, J.L. McLaughlin, P.R. Hanson, Z. Zhuang and T.R. Hoye. *J. Am. Chem. Soc.* **114**, 10203 (1992).

31. (a) I.J. Pachter, R.F. Raffauf, G.E. Ullyot and O.Ribeiro. *J. Am. Chem. Soc.* **82**, 5187 (1960).
(b) T. Kametani, C.V. Loc, T. Higa, M. Koizumi, M.Ihara and K. Fukumoto. *J. Am. Chem. Soc.* **99**, 2306 (1977).
(c) J. Kökösi, I. Hermecz, G. Szász and Z. Mészáros. *Tetrahedron Lett.* **22**, 4861 (1981).

32. D.G. O'Donovan and H. Horan. *J. Chem. Soc.* (C), 2466 (1970).

33. D.F. Barringer, JR., G. Berkelhammer and R.S. Wayne. *J. Org. Chem.* **38**, 1937 (1973).

34. E. Fiedler, H.-P. Fiedler, A. Gerhard, W. Keller-Schierlein, W.A. König and H. Zähner. *Arch. Microbiol.* **107**, 349 (1976).

35. A. Numata, C. Takahashi, T. Matsushita, T. Miyamoto, K. Kawai, Y. Usami, E. Matsumura, M. Inoue, H. Ohishi and T. Shingu. *Tetrahedron Lett.* **33**, 1621 (1992).

36. B.C. Pressman. *Annu. Rev. Biochem.* **45**, 501 (1976).

37. J.F. Hinton and G.L. Turner. *J. Magn. Reson.* **59**, 262 (1984).

38. D.B. Strongman, G.M. Strunz, P Giguere, C.-M. Yu and L. Calhoun. *J. Chem. Ecol.* **14**, 753 (1988).

39. J.F. Grove and M. Pople. *Mycopathologia* **70**, 103 (1980).

40. H. Tomoda, H. Nishida, X.-H. Huang, R. Masuma, Y. K. Kim and S. Omura. *J. Antibiotics* **45**, 1207 (1992).

41. (a) E. Gaumann, St. Naef-Roth and H. Kern. *Phytopathol. Z.* **40**, 45 (1960).
(b) H. Burmeister and R.D. Plattner. *Phytopathology* **77**, 1483 (1987).

42. H. Tomoda, X.-H. Huang, J. Cao, H. Nishida, R. Nagao, S. Okuda, H. Tanaka and S. Omura. *J. Antibiotics* **45**, 1626 (1992).

43. P.C. Anderson, S. Rakhit, C. Yoakim. European Patent Application, Publication No. 443 560, published August 28, 1991.

44. K.H. Domsch, W. Gams and T.-H. Anderson. *Compendium of soil fungi*, Volumn 1, 794.

45. G.C. Papavizas. *Annu. Rev. Phytopathol.* **23**, 23 (1985).

46. R. Andrade, W.A. Ayer and P.P. Mebe. *Can. J. Chem.* **70**, 2526 (1992).

47. (a) J.M. Dickinson, J.R. Hanson and P.B. Hitchcock. *J. Chem. Soc. Perkin Trans.* I 1885 (1989).
(b) N. Claydon, J.R. Hanson, A. Truneh and A.G. Avent. *Phytochemistry* **30**, 3802 (1991).

48. W.D. Ollis and M. Rey. *Tetrahedron* **36**, 515 (1980).